

April 2012

# Mechanical Stimulation Device for Skeletal Muscle Tissue Engineering

Carolynn Elisabeth Ohlson  
*Worcester Polytechnic Institute*

Mary C. McCorry  
*Worcester Polytechnic Institute*

Samuel William Gunnell  
*Worcester Polytechnic Institute*

Sydney Lynn Higginbottom  
*Worcester Polytechnic Institute*

Follow this and additional works at: <https://digitalcommons.wpi.edu/mqp-all>

---

## Repository Citation

Ohlson, C. E., McCorry, M. C., Gunnell, S. W., & Higginbottom, S. L. (2012). *Mechanical Stimulation Device for Skeletal Muscle Tissue Engineering*. Retrieved from <https://digitalcommons.wpi.edu/mqp-all/2251>

This Unrestricted is brought to you for free and open access by the Major Qualifying Projects at Digital WPI. It has been accepted for inclusion in Major Qualifying Projects (All Years) by an authorized administrator of Digital WPI. For more information, please contact [digitalwpi@wpi.edu](mailto:digitalwpi@wpi.edu).



## Mechanical Stimulation Device for Skeletal Muscle Tissue Engineering

A Major Qualifying Project submitted to the faculty of Worcester Polytechnic Institute in partial fulfillment of the requirements for the Degree of Bachelor of Science

Submitted by:

Samuel Gunnell \_\_\_\_\_

Sydney Higginbottom \_\_\_\_\_

Mary Clare McCorry \_\_\_\_\_

Carolynn Ohlson \_\_\_\_\_

Submitted to:

Professor Raymond Page \_\_\_\_\_

Professor Kristen Billiar \_\_\_\_\_

## Abstract

**Abstract—The goal of this project was to create an accurate model for skeletal muscle *in vitro*, with a specific focus to enable mechanical stimulation of the tissue. The project began by creating a list of functions, objectives, and constraints based upon a client needs statement. Conceptual designs were then created and tested for feasibility in order to select components of the final design. The final design includes both a device for mechanical stimulation as well as a method for producing tissue rings that can be placed onto the device.**

### I. INTRODUCTION

The field of skeletal muscle tissue engineering presents clinical promise and offers potential for accurate models of myogenesis and pharmacological therapies. In healthy skeletal muscle tissue, small injuries are constantly repaired by satellite cells that reside in the tissue's basement membrane [1]. When activated by signals released from damaged muscle, these cells are able to differentiate into myoblasts, which then form fused multi-nucleated myofibers [2]. The new tissue becomes vascularized and innervated, restoring function to damaged regions [3]. However, in cases of larger trauma or myopathy, the regenerative capacity of skeletal muscle tissue is severely limited and can result in extensive scarring and reduced functionality [4].

The field of skeletal muscle tissue engineering attempts to address these problems by offering new solutions for culturing and conditioning skeletal muscle in a highly controlled environment *in vitro*. Despite many advances in the field, tissue engineered skeletal muscle has not approached the mechanical properties or resiliency of native skeletal muscle tissue. Successful myogenesis *in vitro* requires an environment that mimics the natural cell niche *in vivo* [5]. This includes a combination of factors involving cytokines, innervation and vascularization, and mechanical stimulation [6]. Powell et al. showed that mechanical stimulation during myotube formation improves fiber diameter, density, and contractibility [6]. Mechanical stimulation is an integral aspect of maintaining the tissue construct over time and is posited to improve penetration of culture medium into the construct [6]. Thus, the purpose of this project is to design a method to consistently enable modeling of skeletal muscle tissue *in vitro* and be amenable to mechanical stimulation.

### II. DEVICE DESIGN

Based on the client needs statement, the team created a list of objectives, constraints, and functions. The primary objectives state that the device should enable modeling of tissue formation *in vitro*, permit the study of skeletal muscle tissue, be consistent/reproducible, and allow for mechanical conditioning of muscle tissue produced.

In order for the device to meet the outlined objectives, it must allow the following functions:

- Able to measure contractile function
- Able to anchor fibers to prevent tissue collapse
- Able to histologically and/or microscopically analyze resulting muscle tissue
- Able to adequately perfuse nutrients to tissue
- Able to electrically stimulate the tissue
- Able to support multiple cell types

- Able to mechanically stimulate the tissue
- Able to control environmental factors and physical components, and
- Able to support both proliferation and differentiation.

These criteria were used to develop four conceptual designs. The feasibility of these designs was evaluated through experimental testing of individual design components. Based on these results, the team was able to draft a final design.

The final design consists of a molding system that is compatible with the mechanical stimulation device (Figure 1). The majority of the device was constructed to fit into a commercially available square tissue culture dish (Figure 1A). Four laser-cut acrylic tracks (Figure 1B) were fixed to the top of the culture dish, in which a separate component is mobile in one direction (Figure 1C). On one end of the slider there are four stainless steel pins that extend downward into the dish that provide the first anchor point for the tissue construct. The second anchoring point is provided by four more pins that extend down from the center of the dish lid and are the stationary anchor points. On the other side of the slider is a notch cut out for the attachment of a magnet. Surrounding the culture dish is a base (Figure 1D), which functions to keep the culture dish stationary and allows for the attachment of a small stepper motor (not shown).

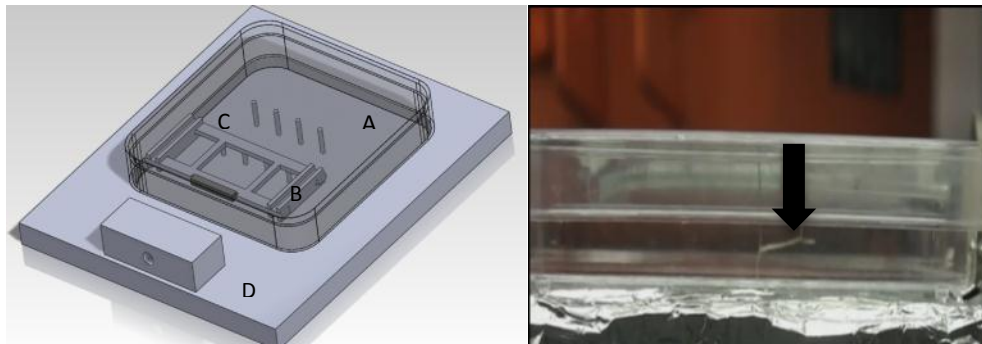


*Figure 1. (left) SolidWorks™ drawing of preliminary design for mechanical stimulation (right) Assembled device with tissue construct (black arrow) mounted on pins*

Another magnet is attached to the end of the actuating arm of the motor and aligned precisely with the magnet inside the culture dish (Figure 1C). When the outside magnet comes into the magnetic field range of the inside magnet, the sliding component will move within the tracts, separating the anchoring pins and stretching the tissue construct. The sliding component retracts when the outside magnet is backed away from the dish by the action of a small spring attached to the lid of the dish. The linear actuator is controlled to create varying cyclic loading protocols using the Arduino™ software.

A molding system was designed for compatibility with the mechanical stimulation device. Carved from polycarbonate, a positive mold of 20 mm long oval rings was machined. To establish preliminary tissue construct formation, molding methods were used as described in Gwyther et al. [8]. The team cast agarose directly into the polycarbonate mold to create a mold of 8 oval rings. Cells seeded into the

agarose mold would form tissue constructs that could be carefully transferred from the mold onto the stainless steel pins in the device for mechanical stimulation.

### III. VALIDATION AND PRELIMINARY RESULTS

Tissue was successfully formed into ring structures using molds with internal diameters of 2, 4, and 6 mm. The oval mold facilitated the formation of oval rings; however the tissue construct broke within 24 hours. The tissue formed by the rings was able to be maneuvered onto the device and mechanically stimulated in the device using Arduino™ software.

The agarose mold permits the study of tissue formation by cell self-assembly or with the aid of extracellular matrix materials such as collagen or fibrin gels [7]. Figure 2 shows C2C12 skeletal muscle tissue ring formation using an agarose mold designed by Gwyther et al. [8]. The left panels in Figure 2 shows that C2C12 can form rings that can be removed and handled. Several cell seeding densities were explored. The top middle panel shows a high seeding density of  $5 \times 10^6$  cells/cm<sup>3</sup> that after 5 days formed a thicker fiber with some myotube formation; however the cells lacked circumferential alignment. The bottom middle panel depicts a lower seeding density at  $2.33 \times 10^6$  cells/cm<sup>3</sup> that after 2 days formed a thinner fiber with improved circumferential cell alignment. The right panel shows that in a 2D system the C2C12s have a much greater myogenic capability than in the 3D ring system. The bottom right image shows a myosin stain which is indicative of myotube formation and C2C12 myoblast differentiation into myocytes. The rings formed in static culture showed minimal myosin expression, likely because the tissue lacked mechanical stimulation to encourage tissue maturation.

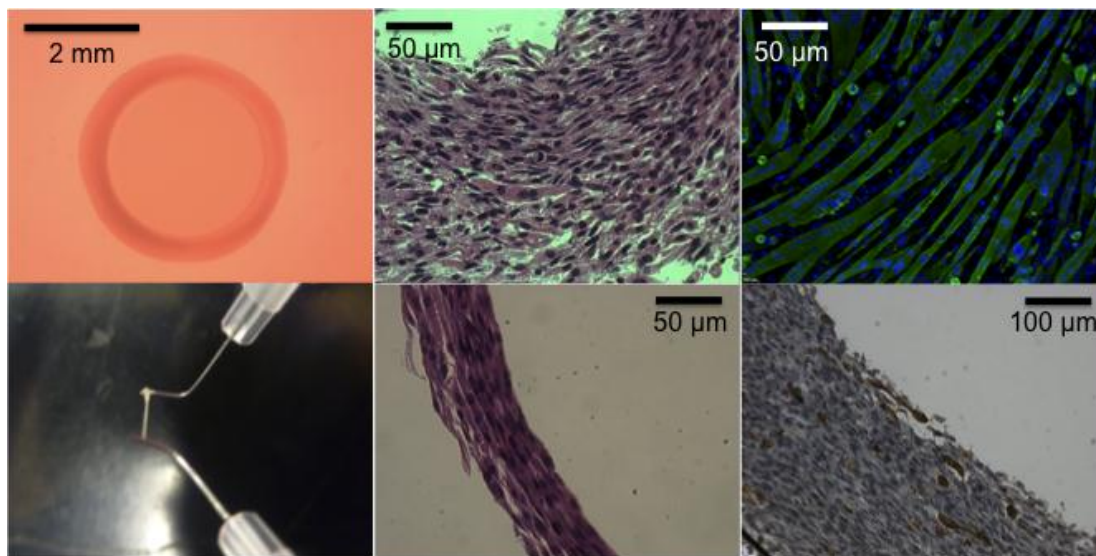


*Figure 2. (top left) C2C12 tissue ring seeded in agarose molds (bottom left) Tissue ring on pins removed from mold (top middle) H&E staining of thick (bottom middle) H&E staining of thin tissue (top right) Myosin (green) and Hoescht (blue) staining of C2C12 cells in 2D culture (bottom right) Myosin (brown) staining of C2C12 3D tissue*

#### IV. CONCLUSIONS AND FUTURE RECOMMENDATIONS

The final design is a feasible, functional device for the mechanical stimulation of developing engineered skeletal muscle tissue that has potential for future improvement and optimization. The team's future recommendations focus on strengthening the initial tissue's mechanical integrity by co-culture with fibroblast cells, which contribute to the structural integrity of skeletal muscle tissue *in vivo*. These cells may strengthen the early tissue by depositing extracellular matrix as the tissue self-assembles in the agarose molds, which would make the tissue easier to handle and more resistant to breaking under the strain of initial contraction. Further development of the device itself may focus on incorporation of electrical stimulation of the tissue, as well as the integrated ability to accurately control and adjust percent strain and tissue diameter. With further development this design has the potential to have a significant impact on the field of skeletal muscle tissue engineering.

#### ACKNOWLEDGEMENTS

Project supported by Worcester Polytechnic Institute Department of Biomedical Engineering and Mechanical Engineering.

#### REFERENCES

- [1] S. B. P. Charge and M. A. Rudnicki. "Cellular and molecular regulation of muscle regeneration." *Physiol. Rev.* 84(1), pp. 209-238. 2004.
- [2] Turner, N., & Badylak, S. "Regeneration of Skeletal Muscle." *Cell and Tissue Research, ePub, in press.* 2011
- [3] S. Ciciliot and S. Schiaffino. "Regeneration of mammalian skeletal muscle: Basic mechanisms and clinical implications." *Curr. Pharm. Des.* 16(8), pp. 906-914. 2010.
- [4] S. Brunelli and P. Rovere-Querini. "The immune system and the repair of skeletal muscle." *Pharmacological Research* 58(2), pp. 117-121. 2008.
- [5] R. W. Ten Broek, S. Grefte and J. W. Von den Hoff. "Regulatory factors and cell populations involved in skeletal muscle regeneration." *J. Cell. Physiol.* 224(1), pp. 7-16. 2010.
- [6] C. A. Powell, B. L. Smiley, J. Mills and H. H. Vandenburgh. "Mechanical stimulation improves tissue-engineered human skeletal muscle." *American Journal of Physiology-Cell Physiology* 283(5), pp. C1557-C1565. 2002.
- [7] A. P. Rago, P. R. Chai and J. R. Morgan. Encapsulated arrays of self-assembled microtissues: An alternative to spherical microcapsules. *Tissue Engineering Part A* 15(2), pp. 387-395. 2008.
- [8] T. A. Gwyther, J. Z. Hu, K. L. Billiar and M. W. Rolle. Directed cellular self-assembly to fabricate cell-derived tissue rings for biomechanical analysis and tissue engineering.
- [9] R. G. Dennis and P. E. Kosnik. "Excitability and isometric contractile properties of mammalian skeletal muscle constructs engineered in vitro." *In Vitro Cellular & Developmental Biology-Animal* 36(5), pp. 327-335. 2000.
- [10] J. Shansky, J. Chromiak, M. Del Tatto and H. Vandenburgh. "A simplified method for tissue engineering skeletal muscle organoids in vitro." *In Vitro Cellular & Developmental Biology-Animal* 33(9), pp. 6

# Table of Contents

<b>Abstract</b>	<b>ii</b>
<b>Table of Contents</b>	<b>vi</b>
<b>Acknowledgements</b>	<b>viii</b>
<b>Authorship</b>	<b>ix</b>
<b>Table of Figures</b>	<b>x</b>
<b>Table of Tables</b>	<b>xii</b>
<b>1: Introduction</b>	<b>1</b>
<b>2: Literature Review</b>	<b>2</b>
2.1: <i>Skeletal Muscle</i>	2
2.1.1: Embryonic Development and Formation of Skeletal Muscle	2
2.1.2: Muscle Tissue	4
2.2: <i>Skeletal Muscle Tissue Regeneration</i>	6
2.2.1: Inflammation	7
2.2.2: Tissue Formation	7
2.2.3: Tissue Remodeling	9
2.3: <i>Clinical Motivation</i>	10
2.3.1: Acute Muscle Trauma	11
2.3.2: Myopathies	12
2.4: <i>Current State of Skeletal Muscle Tissue Engineering</i>	13
2.4.1: Cell Types for Skeletal Muscle Tissue Engineering	14
2.4.2: Recreating the Skeletal Tissue Environment	14
2.4.3: Producing Structural Integrity <i>In Vitro</i>	21
2.5: <i>Literature Review Summary</i>	23
<b>3: Design Process and Strategy</b>	<b>25</b>
3.1: <i>Initial Client Statement</i>	25
3.2: <i>Objectives, Constraints, and Functions</i>	26
3.2.1: Pruned Objectives	26
3.2.2: Constraints	29
3.2.3: Functions	30
3.3: <i>Revised Client Statement</i>	30
<b>4: Design Alternatives</b>	<b>31</b>
4.1: <i>Needs and Functions Analysis</i>	31
4.2: <i>Alternative Designs</i>	32
4.2.1: Design Alternative #1	33
4.2.2: Design Alternative #2	34

4.2.3: Design Alternative #3	35
4.2.4: Design Alternative #4	36
<i>4.3: Feasibility Studies</i>	37
4.3.1: Agarose Molding	37
4.3.2: Magnet Mechanical Stimulation Feasibility	40
<i>4.4: Experimental Methods</i>	42
4.4.1: Cell Culture Maintenance	42
4.4.2: Optimizing Differentiation in Culture	43
4.4.3: Optimizing Tissue Construct Formation	46
<i>4.5: Preliminary Data</i>	48
4.5.1: Optimizing Differentiation in Culture	49
4.5.2: Optimizing Tissue Construct Formation	53
<i>4.6: Preliminary Design</i>	55
4.6.1: Molding System	55
4.6.2: Culture Vessel and Mechanical Stimulation Device	55
<b>5: Design Verification</b>	<b>61</b>
<i>5.1: Mold Designs</i>	61
<i>5.2: Culture Dish Fabrication and Assembly</i>	62
<i>5.3: Base Design and Fabrication</i>	64
<i>5.4: Evaluation of Tissue Constructs</i>	64
<b>6: Final Design</b>	<b>66</b>
<i>6.1: Final Device</i>	66
6.1.1: Final Device Design	66
6.1.2: Final Device Assembly	69
<i>6.2: Final Method for Tissue Construct Formation</i>	70
6.2.1: C2C12 Cell Line	71
6.2.2: Human Skeletal Muscle Primary Cells	71
<b>7: Discussion</b>	<b>73</b>
<i>7.1: Device Discussion</i>	73
<i>7.2: Tissue Discussion</i>	73
<b>8: Conclusions and Recommendations</b>	<b>75</b>
<i>8.1: Device Conclusions</i>	75
<i>8.2: Tissue Conclusions</i>	75
<i>8.3: Device Recommendations</i>	76
<i>8.4: Tissue Recommendations</i>	77
<i>8.5: Impact</i>	77
<b>References</b>	<b>79</b>



## Acknowledgements

We would like to thank the following people for their guidance and support, without which this project could not have been successful:

Raymond Page, Ph.D.

Kristen Billiar, Ph.D.

Tuba Bas, Ph.D.

Lisa Wall, Lab Manager

Sakthikumar Ambady, Ph.D.

Neil Whitehouse, Lab Machinist

Marsha Rolle, Ph.D.

Tracy Gwyther, Ph.D.

Jonathan Grasman

## Authorship

All group members contributed equally to the authorship and editing of this report. Cell culture and tissue experiments were performed by Mary Clare McCorry and Carolynn Ohlson. Device design and construction was performed by Samuel Gunnell and Sydney Higginbottom.

## Table of Figures

Figure 1: Skeletal Muscle Structure .....	5
Figure 2: Satellite Cells and Skeletal Muscle Regeneration (Shi and Garry, 2006) .....	8
Figure 3: From Satellite Cells to New Myofibers (Shi and Garry, 2006) .....	9
Figure 4: Cycle of Chronic Myopathic Muscle Injury and Regeneration vs. Normal Muscle Regeneration (Brunelli, 2008) .....	12
Figure 5: CPK Activity of C2C12 Cells (Lawson et al, 2000) .....	16
Figure 6: Immunofluorescent Images of TESM in Differentiation Media (actin is red, myosin is green, and nuclei are blue) (Gawlitta et al, 2007) .....	17
Figure 7: Vessel Formation for Endothelial Cells Co-Cultured with Mouse Skeletal Myoblasts (Levenberg et al, 2005) .....	18
Figure 8: Cyclic Load Pattern (Powell et al, 2002) .....	19
Figure 9: Light Microscopy of Neural Cells One Week After Plating (Larkin et al, 2006) .....	21
Figure 10: Weighted Objective Tree .....	29
Figure 11: Design Alternative #1.....	33
Figure 12: Design Alternative #2.....	34
Figure 13: Design Alternative #3.....	<b>Error! Bookmark not defined.</b>
Figure 14: Design Alternative #4.....	36
Figure 15: Mold Conceptualization.....	37
Figure 16: Seeding Channel with Missing Post .....	38
Figure 17: Seeding Channel with Post .....	39
Figure 18: Magnetic Track-Slider Experimental Model .....	41
Figure 19: Seeding Density Experiment Schematic .....	44
Figure 20: Population Doubling Time Calculations .....	49
Figure 21: Seeding Density Images .....	50
Figure 22: Fusion Index vs. Seeding Density .....	51
Figure 23: Seeding Timing Images and Nuclei Count.....	52
Figure 24: Ring broken after tissue formation.....	53
Figure 25: H&E Staining of C2C12 Tissue Constructs .....	54
Figure 26: SolidWorks™ drawing of preliminary design for mechanical stimulation .....	56
Figure 27: Bottom of Culture Dish .....	57
Figure 28: Component B Side Profile.....	57
Figure 29: Component B Front Profile .....	57
Figure 30: Component C Top-Down View .....	58
Figure 31: Components B and C .....	58
Figure 32: Component D Stabilizing Base .....	59
Figure 33: Linear Actuating Motor.....	60
Figure 34: Portescap Stepper Can Stack Motor .....	60
Figure 35: SolidWorks representation and image of actual oval-shaped mold.....	61
Figure 36: 2D View of Redesigned Slider .....	63
Figure 37: Assembled base .....	64
Figure 38: Difference in Myosin Expression from 2D to 3D Culture .....	65
Figure 39: Final Design for Mechanical Stimulation Device.....	66
Figure 40: SolidWorks Representation of Layered Acrylic Base .....	67

Figure 41: Lid of the Culture Dish with Attached Pins .....	68
Figure 42: Slider with Mounting Pins and Notch for Magnet .....	68
Figure 43: The Arduino code used for running the stepper motor .....	70

## Table of Tables

Table 1: Key Growth Factors in Skeletal Muscle Regeneration (Ten Broek et al, 2010).....	15
Table 2: Main Objective Pairwise Comparison Chart .....	27
Table 3: Sub-Objectives of Objective 1 Pairwise Comparison Chart .....	27
Table 4: Sub-Objectives of Objective 2 Pairwise Comparison Chart .....	28
Table 5: Sub-Objectives of Objective 3 Pairwise Comparison Chart .....	28
Table 6: Sub-Objectives of Objective 4 Pairwise Comparison Chart .....	28
Table 7: Functions-Means Chart.....	32

## 1: Introduction

The field of skeletal muscle tissue engineering presents clinical promise and offers potential for accurate models of myogenesis and pharmacological therapies. In healthy skeletal muscle tissue, small damages are constantly repaired by satellite cells that reside in the tissue's basement membrane. These cells are able to differentiate into myoblasts, which then form fused multi-nucleated myofibers. The new tissue becomes vascularized and innervated, restoring function to damaged regions. In cases of trauma or myopathy however, the regenerative capacity of skeletal muscle tissue is severely limited, resulting in extensive scarring and reduced functionality.

The field of skeletal muscle tissue engineering attempts to address these problems by offering new solutions for culturing and conditioning skeletal muscle in a highly controlled *in vitro* environment. Despite many advances in the field, tissue-engineered skeletal muscle has not approached the strength or viability seen in native skeletal muscle tissue. This paper reviews the pertinent literature on skeletal muscle formation, structural hierarchy, and mechanisms of regeneration *in vivo*. A detailed discussion of the clinical motivation for tissue engineering skeletal muscle serves as a backdrop for an overview of the current practices, successes, and failures found in the literature. The initial stages of the engineering design process are presented through the lens of this literature review, culminating in the presentation of four conceptual design alternatives aimed to create improved engineered skeletal muscle *in vitro*.

A preliminary design was chosen based upon a series of feasibility studies that evaluated aspects of alternative designs as well as cell culture methods specific to this project's needs. The design was then refined after the collection of preliminary data, and a final design decided upon. The final design successfully provides a platform for the mechanical stimulation, specifically cyclic stretch, of self-assembled skeletal muscle tissue constructs. The following report describes in detail the relevant literature review, design process, conclusions, and future recommendations associated with the completion of this project.

## 2: Literature Review

### 2.1: Skeletal Muscle

The human body is comprised of over 639 skeletal muscles. These skeletal muscles are anchored to bone by tendons and are responsible for skeletal movement such as locomotion and maintaining posture. They are made up of muscle fibers, and as these fibers contract, they create movement of the bone that they are attached to. As a percentage of body mass, an average adult male is made up of 42% skeletal muscle, and an average adult female is 36% skeletal muscle (Standley, 2000). As such, skeletal muscle is a critical player in almost every conceivable aspect of daily life. This section outlines the development and formation of skeletal muscle, the structural hierarchy and components of skeletal muscle tissue, the processes by which skeletal muscle responds to injury or trauma *in vivo*, and the clinical motivations that set the stage for the field of skeletal muscle tissue engineering.

#### 2.1.1: Embryonic Development and Formation of Skeletal Muscle

##### *Skeletal muscle formed by cells derived from somites*

All muscles are derived from the paraxial mesoderm. The paraxial mesoderm is divided along the embryo's length into somites, which correspond to the segmentation of the body. Each of these somites has three divisions which are the sclerotome, dermatome, and the myotome. Sclerotome forms vertebrae, dermatome forms skin and connective tissue, and myotome is responsible for the development of muscle (Neas, 2003).

The myotome, which is the part of the somite responsible for the development of muscles, can be divided into hypaxial and epaxial parts according to an anatomical division of the body and its musculature. The epaxial dermomyotome creates the deep back muscles whereas the hypaxial dermomyotome is responsible for the creation of the rest of the musculature and limbs of the body. From the epithelium of the hypaxial dermomyotome, muscle progenitor cells delaminate and migrate into the limb field to the locations where the dorsal and ventral muscle masses will initially form (Buckingham et al, 2003). It is believed that mesenchymal cells of the respective limb are responsible for providing positional cues to the muscle progenitor cells that accompany that limb. The positioning of the progenitor cells within the epaxial myotome depends on  $\alpha 6\beta 1$  integrin interaction with laminin. This interaction also plays a role in limiting the myogenic potential of cells in the dermomyotome, at the beginning of myogenesis (Schiaffino and Partridge, 2009).

### *Delamination and migration of muscle progenitor cells*

Both delamination and the migration of muscle progenitor cells depend highly on both c-met and Pax3, both of which are myogenic factors. C-met is a tyrosine kinase receptor that interacts with its ligand, HGF (hepatocyte growth factor, also called scatter factor) to line the route of migration for the progenitor cells. Both the receptor and the ligand are essential for the movement of muscle progenitor cells from the somite. In mutant mouse embryos that lack either c-met or the scatter factor, the limbs do not contain skeletal muscle (Buckingham et al, 2003).

The transcription of the c-met gene is dependent on Pax3, a transcription factor characterized by the presence of homeo- and paired domain patterns. On its own, Pax3 is a poor activator and can even repress transcription. However, when a sequence encoding variation of the gene, Pax3-FKHR is added, the complex is complete and the production of hypaxial muscle progenitor cells resumes. Pax3 transcripts are noticeable in presomitic mesoderm and the later effects of this transcription factor on muscle progenitor cells in the somite may be due to the presence of stage and site-specific transcriptional co-activators (Buckingham et al, 2003). Another transcription factor that helps activate migration of progenitor cells from the somite is Lbx1. In mutant embryos that lack Lbx1, muscle progenitor cells delaminate from the dermomyotome but remain near the somite where they may adopt other cell fates. In the forelimb, dorsal muscle masses are especially affected whereas the ventral masses migrate correctly (Schiaffino and Partridge, 2009).

### *Proliferation and differentiation in the limb*

Cells that migrate from the somite have not yet experienced the myogenic determination factors that control myogenic cell differentiation, which is characterized by the activation of muscle genes and the formation of muscle fibers. The genes that regulate this process are myogenin, MyoD, Myf5 and Mrf4. Myf5 is transcribed before the start of myogenesis, in cells located at the edges of the dermomyotome, which will ultimately delaminate to form the skeletal muscle of the myotome. MyoD is activated later in hypaxial and then in epaxial progenitor cells which contribute to the mature myotome. Mice that lack Myf5 have progenitor cells that fail to correctly locate and therefore become incorporated into other tissues such as cartilage and bone (Schiaffino and Partridge, 2009). The function of Mrf4 as a myogenic determination factor is consistent with its role in efficiently re-modeling chromatin to open it for transcription during myogenesis (Schiaffino and Partridge, 2009). Once the early myotome is formed, Mrf4 is no longer expressed in myogenic progenitor cells and its function is restricted to myogenic differentiation.



When Myf5 alone is present, myogenesis is delayed, suggesting that the level of Myf5 is unimportant in initiating myogenesis. In the absence of MyoD, myogenesis takes place normally. Although, in the limb for example, there is a delay which could come from the fact that initial levels of Myf5 are not enough to trigger differentiation of myoblasts to myocytes (Schiaffino and Partridge, 2009). The activation of these genes inside the limb depend on signaling molecules such as Wnts and Sonic hedgehog that are produced by the dorsal surface ectoderm and the zone of polarizing activity. Before skeletal muscle forms and most likely before and after the activation of Myf5 and MyoD, muscle progenitor cells undergo proliferation in the limb. Although MyoD was not detected in dividing myoblasts in chick embryos, in the mouse, both Myf5 and MyoD are expressed in proliferating muscle cells and most likely play a role in cell cycle regulation (Buckingham et al, 2003).

As the development process continues, muscle masses divide to form the specific muscles of the body. As with the migrating progenitor cells, these muscle masses will develop depending on their environment and may contain different proportions of slow and fast fibers. However, there is no noticeable difference in their gene expression.

### 2.1.2: Muscle Tissue

#### *Structural Hierarchy*

A myocyte, also called a muscle cell, is simply the cell type that makes up the contractile fibers of muscle tissue. There are various forms of myocytes which coincide with the different types of muscles; smooth muscle cells, cardiac muscle cells, and skeletal muscle cells. In skeletal muscle, these myocytes, which arise from the embryonic muscle progenitor cells called myoblasts, are the starting point of the structural hierarchy within the muscle. The fusion of these myoblasts creates myocytes, which therefore contain multiple nuclei (each nucleus originating from a single myoblast).

A myofibril (which means “muscle thread”) is a string of sarcomeres arranged in series. Sarcomeres are composed of contractile filaments called myofilaments. There are two major sets of contractile filaments within the sarcomere: the proteins myosin and actin. These microscopic filaments produce muscle shortening, and the interdigitated patterns of these filaments give the muscle its striated appearance. The myofibrillar diameter is about 1  $\mu\text{m}$ , which means that thousands can be packed into a single muscle fiber. The total number of sarcomeres within a fiber depends on the muscle fiber length and diameter. These myofibrils are arranged in parallel to each other to make up the muscle fiber.

Surrounding the muscle fiber is the sarcolemma, which consists of the basement membrane and plasmalemma. The plasmalemma is the plasma membrane that immediately surrounds the muscle fiber and functions as both an anatomical barrier and a selective barrier between the cellular contents and the surrounding connective tissue. Immediately surrounding the sarcolemma is the basement membrane, composed of the basal lamina and the reticular lamina. The functions of the basement membrane involve providing mechanical support to the cells and providing a scaffold for cells during the development and regeneration processes. Between the basal lamina and the plasmalemma lie satellite cells, which are the stem cells responsible for muscle regeneration.

Groups of muscle fibers are surrounded by a connective tissue covering called the perimysium and are arranged in bundles which are called fascicles. These fascicles are bundled together and surrounded by more connective tissue called the epimysium to form the whole muscle, the structure of which is summarized in Figure 1 below (Leiber, 1999).

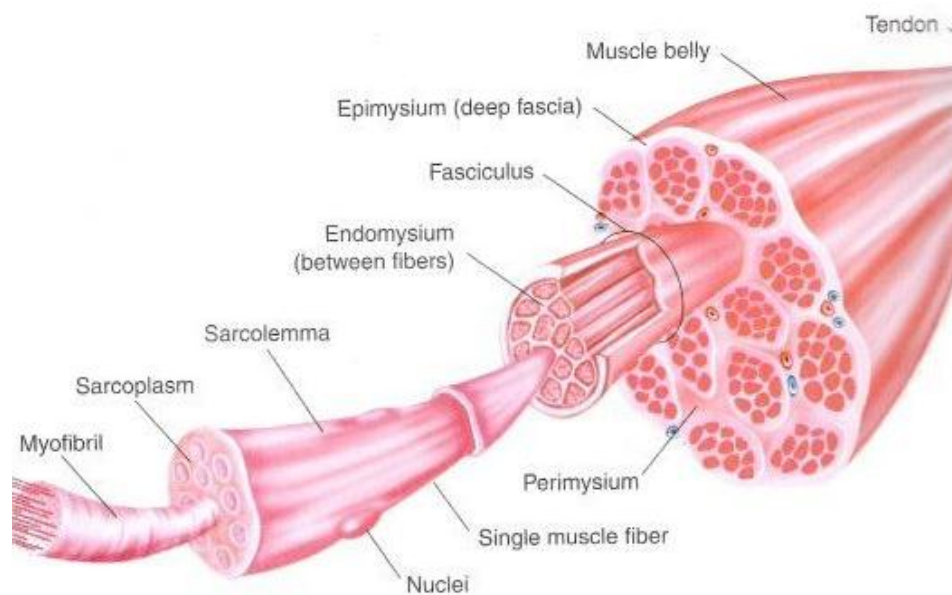


Figure 1: Skeletal Muscle Structure

### ***Extracellular Matrix (ECM)***

Although skeletal muscle formation usually focuses on actin and myosin, an important factor in the growth of muscle is the network of macromolecules, called the extracellular matrix (ECM). The ECM is a part of three connective tissue layers surrounding the muscle fibers: the endomysium, the perimysium, and the epimysium (Velleman, 2002). The epimysium is a layer of connective tissue that

surrounds the entire muscle, the perimysium surrounds a fascicle, or bundle of myofibers, and the endomysium surrounds individual myofibers. ECM is a dynamic structure that regulates cell behavior through the interaction of ECM molecules with each other, the interaction with growth factors, and through cell-ECM signal transduction pathways. This scaffold supports cell attachment, spreading, proliferation, migration and differentiation.

The specialized molecules of the ECM are comprised of three classes: proteins, glycosaminoglycans (GAGs), and proteoglycans. The gel that fills the extracellular space is composed of GAGs, which are polysaccharide chains. Most GAGs are covalently attached to a protein core to form proteoglycans (Saltzman, 174). Some typical glycosaminoglycans that attach to the proteoglycan central core protein are chondroitin sulfate, dermatan sulfate, heparan sulfate and keratan sulfate (Velleman, 2002). There are two types of proteins within the ECM: structural and adhesive. The structural proteins include collagen, which provides strength, and elastin, which provides elasticity. Of the at least 19 collagens with tissue-specific distributions, skeletal muscle ECM is composed of both collagen type I and collagen type III (Velleman<sup>2</sup>). These collagens are fibrillar in nature and contain a single triple-helical domain consisting of three separate peptide chains. These three chains wrap around each other to form an alpha helix and provide mechanical support to the muscle tissue.

Almost all of the proteins within the ECM are proteoglycan, which means they have short chains of carbohydrates attached to them. These glycoproteins facilitate the adhesion of cells to collagen. Adhesive proteins such as fibronectin and laminin help to bind the other matrix components together and facilitate attachment of cells to the ECM (Saltzman, 174). Fibronectins bind to cells via receptors on the cell membrane known as integrins. These integrins can bind to laminins, which are proteins that assemble with collagen type IV to form networks within the basement membrane (Velleman<sup>2</sup>).

## **2.2: Skeletal Muscle Tissue Regeneration**

Skeletal muscle has a remarkable regenerative capability and can often return to complete functional health post-injury, especially in cases where the muscle is healthy prior to injury and sustains little to no volumetric tissue loss as a result of the injury. This regenerative process is generally recognized to occur in three overlapping phases: 1) inflammation, 2) tissue formation, and 3) tissue remodeling. Muscle satellite cells, or quiescent progenitor cells, have recently been identified as the driving players in skeletal muscle regeneration throughout these three phases. The following is an overview of the mechanisms of skeletal muscle regeneration as characterized by these three phases.

### 2.2.1: Inflammation

The first phase of skeletal muscle regeneration is inflammation, which occurs immediately following injury. This phase is characterized by the necrosis of injured myofibers and the subsequent inflammatory response (Turner and Badylak, 2011). Skeletal muscle injury results in ruptured myofibers, which release proteases that then rapidly degrade the damaged fibers (Brunelli and Rovere-Querini, 2008). To prevent these proteases from degrading the undamaged fibers surrounding the site of the injury, the tissue forms a contraction band of cytoskeletal components to isolate them in the area of the injury (Turner and Badylak, 2011).

The release of these proteases and other cellular signals from ruptured myofibers also works to recruit macrophages, which drive the inflammatory response. Macrophages play a dual role in skeletal muscle regeneration: first to promote inflammation, and later to support satellite cell proliferation and differentiation (Brunelli and Rovere-Querini, 2008). The first population of macrophages arrives at the site of the ruptured myofibers immediately following injury and is pro-inflammatory. As these macrophages move to the site of the injury, they interact with nearby satellite cells to increase chemotaxis to the site of the injury. They also secrete pro-inflammatory factors such as TNF- $\alpha$  and IL-1 $\beta$  to recruit more macrophages which clear the debris of damaged myofibers by phagocytosis (Grefte, 2007).

The second population of macrophages, which arrives after 24 hours, begin scaling down the inflammation phase of skeletal muscle regeneration. These macrophages secrete anti-inflammatory factors as well as cytokines such as IL-10 that function to upregulate proliferation and differentiation of satellite cells (Grefte et al, 2007). Thus, macrophages not only remove the debris of degraded myofibers, but also promote the next step of skeletal muscle regeneration: tissue formation.

### 2.2.2: Tissue Formation

The second phase of skeletal muscle regeneration- tissue formation- begins as macrophages finish clearing the debris of damaged myofibers and scale down the inflammatory response. This phase (summarized in Figure 2) is characterized by satellite cell recruitment, proliferation, and differentiation, leading to formation of new skeletal muscle tissue (Turner and Badylak, 2011).

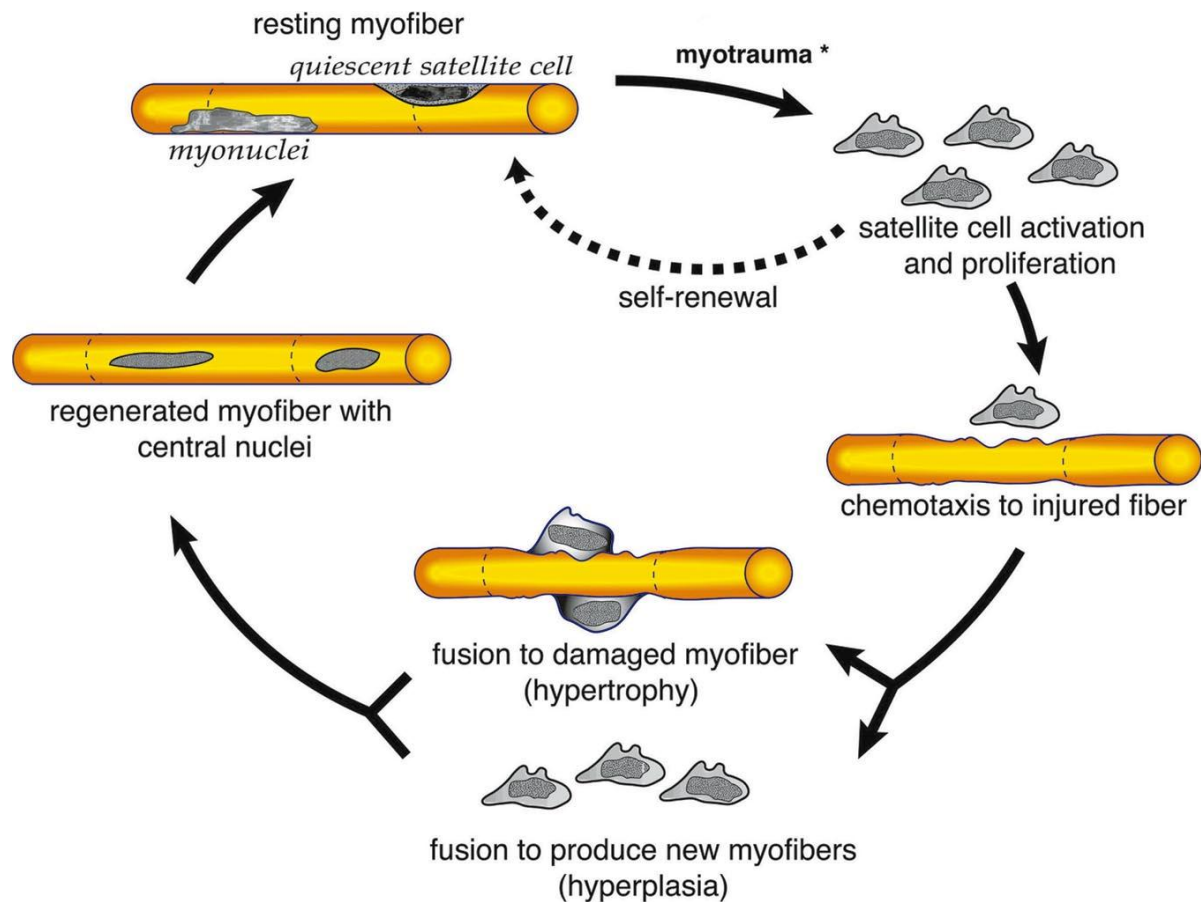


Figure 2: Satellite Cells and Skeletal Muscle Regeneration (Shi and Garry, 2006)

As the second population of macrophages arrives at the site of the injury during the inflammatory phase, they also secrete chemotactic factors to recruit quiescent satellite cells that are associated with the damaged muscle fiber to the injury from their niches between the basal lamina and sarcolemma (Ciciliot et al, 2010). If the basal lamina has been damaged as a result of the injury, satellite cells will migrate from neighboring muscle fibers to repopulate the regenerating myofiber. These cells are then activated by signals released from the macrophages (such as nitric oxide production from debris breakdown) and growth factors such as FGF, HGF, IGF-I, IGF-II, TGF- $\beta$ , and IL-6 (Charge and Rudnicki, 2004). Once these cells are recruited to the site of the injury and are activated from their quiescent state, they proliferate very rapidly (Shi and Garry, 2006). This activity is heavily regulated by interaction with macrophages and through the Notch signaling pathway (Ciciliot et al, 2010) and

generally occurs more than 24 hours after the injury, once the debris is completely cleared and most inflammation has subsided (Brunelli and Rovere-Querini, 2008).

As the satellite cells near the end of this rapid proliferation, they generally follow one of two paths: differentiation into myoblasts (committed myogenic precursors) or a return to the quiescent state (Ciciliot et al, 2010). The new satellite cells that return to a quiescent state remain undifferentiated and serve to maintain the satellite cell population for future regeneration (Brunelli and Rovere-Querini, 2008). Differentiation of the rest of the newly formed satellite cells is regulated in part by a switch from the Notch signaling pathway to the Wnt signaling pathway (Ciciliot et al, 2010). Premature Wnt signaling can lead to early differentiation when there are not yet enough myoblastic cells produced to regenerate the injured skeletal muscle tissue (Ciciliot et al, 2010). Once differentiated, myoblasts either fuse together to form new myofibers or fuse to damaged myofibers to repair them (Brunelli and Rovere-Querini, 2008). These new and repaired myofibers together form regenerated muscle tissue, as shown in Figure 3 below.



Figure 3: From Satellite Cells to New Myofibers (Shi and Garry, 2006)

### 2.2.3: Tissue Remodeling

The regenerated skeletal muscle tissue formed from new and repaired myofibers is not yet fully mature, however, and must still undergo extensive remodeling to become fully functional skeletal muscle tissue. This occurs in the third and final phase of regeneration, which is characterized by the reorganization of myofibers, the remodeling of any scar tissue that may be present, and the restoration of muscle function (Turner and Badylak, 2011). This phase begins after the satellite cells have differentiated and fused into myofibers, as these fibers then align and fuse with one another to become muscle tissue. As this occurs, the myofibers begin to mature into contractile, functioning muscle.

Muscle maturation is characterized mainly by an increase in fiber size (diameter) and by the movement of nuclei from the center of muscle fibers to the periphery (Grefte et al, 2007). In order to

become fully functionally mature, muscle tissue must also be revascularized, reinnervated, and aligned to fully integrate with surrounding muscle tissue.

Revascularization, or the reestablishment of blood supply, is one of the major limiting factors in skeletal muscle regeneration, as the new and repaired myofibers need a source of nutrients and oxygen to survive (Turner and Badylak, 2011). The myoblasts that fuse to form myofibers are unable to survive further than approximately 150 $\mu$ m from a blood supply, as the nutrients and oxygen necessary cannot diffuse through tissue thicker than this (Turner and Badylak, 2011). Thus, fully mature skeletal muscle tissue needs vascular support to ensure tissue survival and to allow full regeneration.

Reinnervation, or the reestablishment of neuronal connections, is another important factor in maturing skeletal muscle tissue. Regeneration can take place up to the end of the second phase without neuromuscular connections, but they are necessary for any further growth and maturation of myofibers (Ciciliot et al, 2010). If these neuromuscular connections are not made as or soon after the tissue is formed, the newly regenerated muscle will atrophy, thus resulting in another injury and need for further regeneration (Turner and Badylak, 2011). Neuromuscular junctions are so important to skeletal muscle tissue maturation because they not only provide functional control, but also chemical cues that support fiber alignment, fiber type (fast or slow twitch) and fiber diameter (Turner and Badylak, 2011).

The last major factor in regenerating mature skeletal muscle tissue is remodeling of the tissue to fully integrate it with existing muscle, as well as to restore full contractile function (Ciciliot et al, 2010). In this process, the basal lamina of the tissue is repaired and used by myofibroblasts to align the regenerated myofibers (Turner and Badylak, 2011). These myofibroblasts also replace the temporary matrix that is quickly laid down during the tissue formation phase with a permanent matrix that will allow the regenerated tissue to fully mature (Grefte et al, 2007). This is the last step to complete skeletal muscle regeneration, and ends the tissue remodeling phase. Through the regenerative process described above, injured skeletal muscle can regain its functionality and return to healthy tissue, exemplifying a regenerative capacity rivaled by very few other tissues.

## **2.3: Clinical Motivation**

The regeneration of skeletal muscle tissue is a closely controlled, finely orchestrated process that, when completed successfully, has the potential to restore injured muscle to its original functional capacity. Through the regenerative phases of inflammation, tissue formation, and tissue remodeling, injured muscle can often repair itself from a variety of types of damage. However, there are limits to the

natural regeneration of skeletal muscle tissue, and it is in these limits that the need for a model of skeletal muscle regeneration and a clinical product to replace muscle tissue that cannot be regenerated becomes clear.

Skeletal muscle tissue has a vast regenerative capacity; even with normal activity, approximately 1-2% of muscle volume is regenerated weekly in healthy individuals (Charge and Rudnicki, 2004). However, muscle is also very susceptible to injury, either as a result of direct trauma or as a result of myopathies (Charge and Rudnicki, 2004). If these injuries remain unrepaired or regenerate incompletely, they can lead to volumetric muscle loss (atrophy), loss of contractile function, and in extreme cases, even death (Charge and Rudnicki, 2004). There are numerous cases where the limits of natural skeletal muscle regeneration can lead to these effects, many of which fall under two categories: chronic muscle disease (myopathies) and acute muscle trauma.

### **2.3.1: Acute Muscle Trauma**

Acute muscle trauma most often occurs in the form of contusions or strains and tears, and is commonly seen in combat injuries, in sports injuries, or in accidents. Contusions are the result of an external blow, and in severe circumstances can lead to swelling and bleeding that cuts off blood flow to muscle tissue and causes tissue damage. Strains occur after repeated muscle contractions that produce excessive forces on muscle tissue that lead to the rupture of myofibers and blood vessels and potentially damage to the basal lamina, inhibiting regeneration. Tears are extreme strains where the muscle tissue actually tears apart on a major scale, resulting in swelling of the tissue and some immediate loss of muscle function.

The ability of skeletal muscle tissue to regenerate after an acute trauma injury is diminished from the regenerative capability of healthy tissue, and is largely dependent on the type and severity of the injury. If more than 20% of the muscle's mass is lost, the regenerative capacity of that muscle is severely limited and will often fail to repair the injury, leading to a buildup of scar tissue and potential loss of function (Turner and Badylak, 2011). In these cases, the remaining muscle simply cannot produce enough new myofibers quickly enough to repair the injury. Damage to the basal lamina can also occur in traumas, which further limits regeneration (Turner and Badylak, 2011). Even in less severe traumas, regeneration is not always complete.

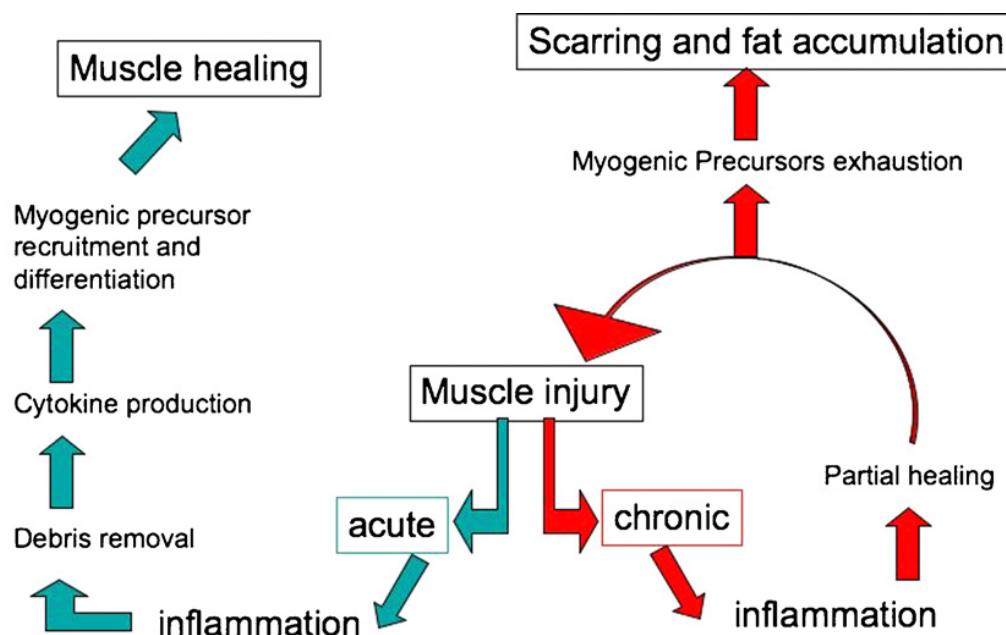
In cases of severe muscle trauma where the skeletal muscle is not able to regenerate completely, the current standard of care is surgery to transfer vascularized tissue to the injured area and potentially restore partial muscle function. In serious trauma, such as that seen in combat injuries,



amputation is often the only option. Even when surgery can be used to partially return function to the injured muscle, it cannot be used to regenerate tissue from volumetric loss, and also represents a decrease in function for the donor as well as the recipient sites (Turner and Badylak, 2011). Patients with severe muscle trauma are often left with physical handicaps, which can have major negative impacts both physically and psychologically. Thus, there is a need for clinical applications that would support skeletal muscle regeneration.

### 2.3.2: Myopathies

The second major cause of skeletal muscle injury is muscle disease, or myopathy. Many myopathies result in chronic muscle injuries that cannot heal completely due to a number of factors, as shown in Figure 4 below.



Schematic representation of the events occurring following acute (left) or chronic (right) muscle injury.

**Figure 4: Cycle of Chronic Myopathic Muscle Injury and Regeneration vs. Normal Muscle Regeneration (Brunelli, 2008)**

The most common category of myopathies is muscular dystrophies, which are characterized by repeated cycles of muscle injury and regeneration. Regeneration in patients with muscular dystrophies is incomplete, however, and results in scattered and misaligned myofibers that do not mature fully and do not regain full contractile function (Ciciliot et al, 2010). Over time, the regenerative capacity of the muscle diminishes as the satellite cell population becomes depleted, and more and more fat and scar

tissue is formed with each new muscle injury that occurs (Brunelli and Rovere-Querini, 2008). This leads to an overall decrease in functional muscle mass and an increase in non-functional scar tissue. Many dystrophies are genetic, and patients often only live until their teens before becoming wheelchair-bound and until their early twenties before the continuous loss of muscle mass impairs cardiovascular and pulmonary function and results in death (Muscular Dystrophy Association, 2011).

Patients with muscular dystrophies and other myopathies are generally unable to completely regenerate muscle tissue on their own, which depletes the muscle's population over time until scar and fat accumulates faster than new skeletal muscle tissue (Brunelli and Rovere-Querini, 2008). A clinical application that supported muscle regeneration in these patients could not only prolong their lives, but also potentially increase the quality of their lives. The need for a model of skeletal muscle regeneration is also present, as it could provide further insight into the regenerative process, how myopathies arise, and how to correct them.

The clinical motivation for generating tissue engineered skeletal muscle, both to replace lost or damaged tissue and to serve as an *in vitro* model of skeletal muscle formation and function, has clearly been recognized in the scientific community. The field of tissue engineering has traditionally employed stem/progenitor cells, scaffolds, and biologic factors to attempt to approximate skeletal muscle tissue *in vitro* (Turner and Badylak, 2011). Such a model that recapitulates skeletal muscle regeneration as it occurs *in vivo* has potential applications in the study of myopathies, the evaluation of drug performance and effect on muscle regeneration prior to use *in vivo*, and further study of muscle regeneration. However, the promise of tissue engineered models and clinical applications of skeletal muscle also comes with many limitations and challenges. The next section includes a comprehensive overview of the successes and failures in the state of the art in creating tissue engineered skeletal muscle, focusing on the application relevant to this project, which is recapitulating skeletal muscle *in vitro*.

## 2.4: Current State of Skeletal Muscle Tissue Engineering

The clinical motivation described above has made tissue engineered skeletal muscle (TESM) a heavily researched topic in the last ten years. Researches have had partial success in achieving TESM *in vitro* through many techniques and methods. A thorough review of the current state of the art in TESM was conducted. The following chapter describes the cell types used, techniques to mimic the *in vivo* environment, and materials used for scaffolding.

### 2.4.1: Cell Types for Skeletal Muscle Tissue Engineering

Researchers studying TESM have used various types of cells in their experiments. These cell types include muscle satellite cells, myoblasts, C2C12 myoblasts, pericytes, embryonic stem cells (ESC), and CD133<sup>+</sup> cells. Although ESCs can differentiate into skeletal myocytes, they have the potential to differentiate into any other type of cell (Camargo et al., 2003). Many research groups have had success with C2C12 and satellite cells (Stern-Straeter et al., 2007).

C2C12, a murine myoblast cell line, have been extensively used for 3-dimensional (3D) TESM. Previous studies showed that C2C12 cells have a high proliferation rate and respond well to tissue culture experiments (Gawilitta et al., 2007). Using C2C12s for TESM is often preferred to other cell lines because they allow for stable genetic modifications to test specific gene function and show consistency in results (Khodabukus et al., 2007). Similar to satellite cells in the body, C2C12 cells are able to differentiate *in vitro* and form myotubes (Gawilitta et al., 2007). In addition to myotubial formation, C2C12 cells undergo myofibrillogenesis to form a contractile apparatus and can therefore respond to electrical and mechanical stimuli (Gawilitta et al., 2007).

Primary, non-immunogenic satellite cells are a preferred source for the study of TESM (Stern-Straeter et al., 2007). Using a simple surgical biopsy, satellite cells can be harvested and cultured *in vitro* (Beier et al., 2006). Similar to C2C12 cells, satellite cells have the ability to proliferate, differentiate, and fuse into multinucleated skeletal muscle fibers (Stern-Straeter et al., 2007).

### 2.4.2: Recreating the Skeletal Tissue Environment

When culturing muscle tissue it is essential to mimic the *in vivo* environment. Three main factors have been identified as crucial in the *in vivo* environment: (1) growth factors, (2) vascularization, (3) mechanical stimulation, and (4) electrical stimulation (Powell et al., 2002). Many researchers have evaluated each of these factors and found that TESM yields more comparable results with improved mechanical and electrical stimulation alongside growth factors added with appropriate timing during the tissue formation process.

#### *Growth Factors and Proteins That Complement Skeletal Muscle Tissue Engineering and Distribution*

Closely mimicking the growth factors and signaling process involved in skeletal muscle formation *in vivo* is essential for success in growing these tissues *in vitro*. Table 1 shows a summary of the important growth factors involved in skeletal muscle formation. In natural regeneration these factors

are typically released by immune cells, muscle cells, or components in the extracellular matrix (ECM) following an injury (Ten Broek., 2010).

Table 1: Key Growth Factors in Skeletal Muscle Regeneration (Ten Broek et al, 2010)

Growth factor	Producing cell type	Proliferation/ differentiation	Function	Literatures
HGF	Active immune cells + vasculature + ECM	+/+	Induces quiescent SC activation	Allen et al. (1995), Suzuki et al. (2002), Tatsumi et al. (1998, 2001)
Basic FGF	Active immune cells + vasculature + autocrine + ECM	+/+	Up-regulated during regeneration, specific role is unclear	Allen and Boxhorn (1989), Doumit et al. (1993), Haugk et al. (1995), Robertson et al. (1993)
IGF-1	Active immune cells + vasculature + autocrine + ECM	+++	Highly mitogenic for myoblasts and promotes cell survival	Adams and McCue (1998), Allen and Boxhorn (1989), Doumit et al. (1993), Haugk et al. (1995), Menetrey et al. (2000), Sato et al. (2003)
IGF-2	Active immune cells + vasculature + autocrine	+/+	Up-regulated after IGF-1 up-regulation, and has a small contribution in myoblast proliferation/differentiation	Doumit et al. (1993), Haugk et al. (1995)
VEGF	Variety of cell types, up-regulated during hypoxia	+/?	Stimulates angiogenesis	Doumit et al. (1993), Gowdak et al. (2000), Springer et al. (1998)
PDGF-AA, PDGF-BB	Active immune cells + endothelial cells	-/+, +/-	Regulate proliferation/differentiation in opposite ways and support angiogenesis	Doumit et al. (1993), Robertson et al. (1993)
Myostatin	Circulation + autocrine	-/-	Maintains SC quiescence	Amthor et al. (2002), McCroskery et al. (2003), McPherron and Lee (1997)
TGF- $\beta$ 1 and TGF- $\alpha$	Active immune cells + autocrine	-/-	Prevents myoblast differentiation and recruitment	Allen and Boxhorn, (1989), Haugk et al. (1995), Robertson et al. (1993)

The ECM proteins have been shown to play a pivotal role in the formation of new muscle tissue. Laminin is a protein located in the basement membrane of the muscle fiber (Kroll et al., 1994). Studies have shown that laminin protein promotes myoblast adhesion, migration, proliferation, and myotube formation (Kroll et al., 1994). Additionally in a study conducted by Vachon et al., they showed that cells not expressing laminin or merosin, a laminin variant, did not fuse to form myotubes. However once the proteins were added into the culture medium cells began to fuse and form multinucleated myotubes (Vachon et al., 1996). Vachon et al.'s studies indicated the merosin increases stability and prevents apoptosis of C2C12 cells *in vitro*. Studies using fibronectin supplement in TESM showed that fibronectin promotes the adhesion and proliferation of myoblasts, however in contrast to laminin, it inhibits the differentiation of myoblasts into fused multinucleated myotubes (Von der Mark et al., 1989).

A study conducted by Lawson et al. compared the effects of BSA (bovine serum albumen), collagen I, collagen IV, laminin, and fibronectin on muscle formation. Differentiated C2C12 cells were applied to flasks coated with BSA, collagen I, collagen IV, laminin, and fibronectin and treated with 2% horse serum (HS) or AIM V medium (medium contains L-glutamine, streptomycin sulfate, and gentamicin sulfate). For cells plated in 2% HS, C2C12 cells plated on collagen IV and laminin showed significantly higher levels of CPK (creatine phosphokinase, an enzyme present in tissue with high

utilization of ATP) activity; see Figure 5 below. This study indicated that the presence of laminin and collagen IV significantly improves muscle differentiation (Lawson et al., 2000).

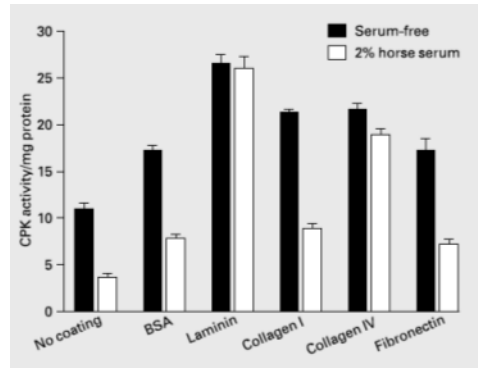


Figure 5: CPK Activity of C2C12 Cells (Lawson et al, 2000)

Growth factors have also been shown to improve myotube formation *in vitro*. IGF has been identified in several studies to have a profound impact on skeletal muscle growth by promoting the proliferation and differentiation of stem cell derived myoblasts (Ten Broek., 2010). A typical method for inducing differentiation in C2C12 muscle cells is by switching from fetal bovine serum (10-20% FBS) to horse serum (1-10% HS) in the medium (Gawlitta et al., 2007). In an attempt to reduce the inconsistency in results Gawlitta et al. experimented with replacing the serum in the media with additives and growth factors such as insulin or insulin like growth factors (IGF). C2C12 cells were cultured with growth media consisting of L-glutamine, 15% FBS, 2% 4-(2-hydroxyethyl)- 1-piperazineethanesulfonic acid, 1% non-essential amino acids, and 0.5% gentamicin. At passage number fourteen the cells were seeded onto the scaffolds at  $4.9 \times 10^6$  cells/mL concentration and exposed to five different growth media. Gawlitta et al. experimented with different combination of horse serum (HS), IGF-1, and Ultrosor G. Ultrosor G is a commercially produced serum substitute that has more defined contents than HS. The comparative results of this study are shown in Figure 6 below, which features immunofluorescent images of TSM in differentiation media containing Ultrosor G (DMU), IGF-1 (DMI), both Ultrosor G and IGF-1 (DMUI), horse serum (HS), or HS with IGF-1 (HSI). The study showed that 2% HS supplemented with IGF-I produced cultures with the highest creatine phosphate levels, indicating myoblast fusion and differentiation into myotubes, HSI in Figure 6 (Gawlitta et al., 2007). IGF-1 by itself could not induce differentiation; however, when combined with Ultrosor G or HS it could induce differentiation at an accelerated rate compared to HS by itself (Gawlitta et al., 2007).

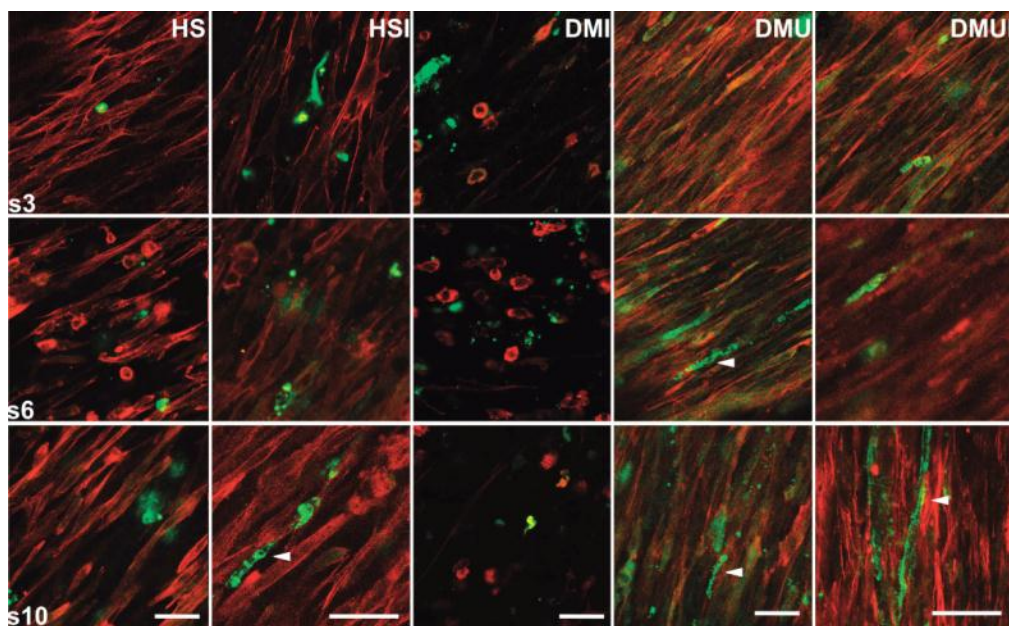


Figure 6: Immunofluorescent Images of TESM in Differentiation Media (actin is red, myosin is green, and nuclei are blue) (Gawlitta et al, 2007)

### *Vascularization of TESM*

In natural skeletal muscle, there is an abundant supply of blood to the muscle fibers. Blood vessels are necessary for the transport of specific chemical signals, growth factors, oxygen, and nutrients. Some groups used matrixes or genetically altered myoblast cells to deliver vascular growth factors (therapeutic angiogenesis) (Von Degenfeld et al., 2003). Clinical investigations indicate that angiogenic factors such as, prototypic vascular endothelial growth factor (VEGF) and basic fibroblast growth factor (bFGF), can improve blood flow to ischemic regions as well as induce angiogenesis (Zisch et al., 2003). Angiogenic factors including VEGF and bFGF can be delivered in a controlled fashion using natural and synthetic polymer matrices (Zisch et al., 2003). Biopolymers have become popular for this application because they protect the protein from external factors as well and preserve the growth factor profile, and respond to natural release mechanisms of the ECM (Zisch et al., 2003). Other methods for vascularization include forming the TESM within an arterio-venous loop or femoral artery, or genetically altering donor cells (myoblasts expressing VEGF) (Zisch et al., 2003).

In a study conducted by Levenberg et al., they co-cultured mouse myoblasts with human embryonic/umbilical vein endothelial cells and seeded them to scaffolds composed of PLLA (poly-L lactic acid) and PLGA (polylactic-co-glycolic acid). After two weeks the myoblasts had differentiated, fused and



aligned into multinucleated myotubes. Concurrently, the endothelial cells formed tubular formations through the scaffold between partially aligned myotubes, see Figure 7 (Levenberg et al., 2005). The addition of endothelial cells to the culture showed expression of vascular endothelial growth factor (VEGF). They also showed that adding fibroblasts to the co-culture resulted in increased expression of VEGF. VEGF functions to stimulate vasculogenesis and angiogenesis to create and repair blood vessels.

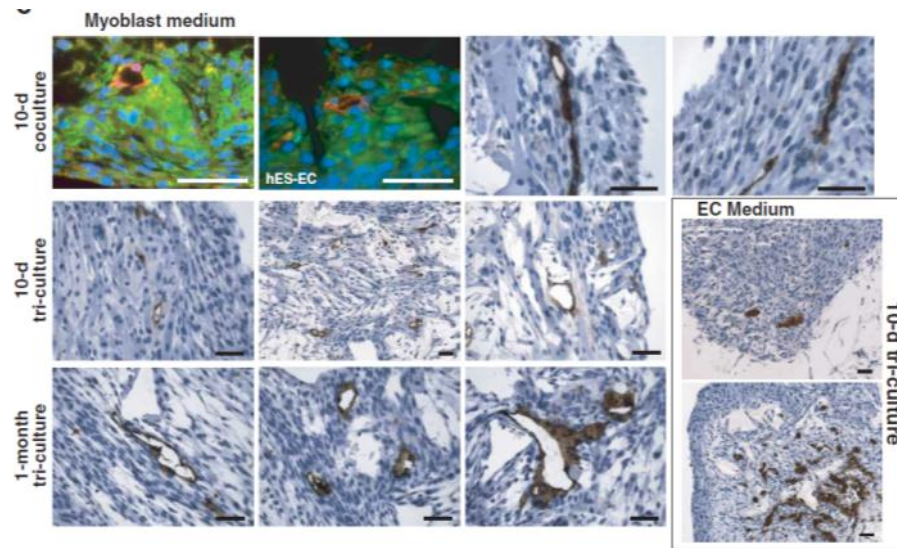


Figure 7: Vessel Formation for Endothelial Cells Co-Cultured with Mouse Skeletal Myoblasts (Levenberg et al, 2005)

### ***Mechanical Stimulation of TESM***

Several studies have demonstrated the positive effects of mechanical stimulation on tissue-engineered skeletal muscle produced *in vitro*. According to Powell et al., ideal myogenesis involves some combination of nutrition, hormones, nerve innervation and exercise. Mechanical stimulation of tissue-engineered constructs attempts to mimic the bone growth and exercise that help to direct myogenesis *in vivo*. While mechanical stimulation is just one part of ideal myogenesis, some of its specific benefits have been widely discussed in the literature. Mann et al. showed that mechanical stimulation has a beneficial influence on gene expression, protein synthesis, and total RNA/DNA content. Other studies focused primarily on morphology, revealing that mechanical stimulation improves myofiber diameter and density (Powell et al., 2002; Moon et al., 2008). One documented phenomena in this aspect of skeletal muscle tissue engineering is that muscle fibers tend to align in the direction of an uniaxial strain (Liao and Zhou, 2009). This alignment is one of the most critical factors in assessing overall functionality of the engineered tissue (Koning, 2009). Additionally, as demonstrated by Powell et al., skeletal muscle

tissue in static culture becomes stiffer over time, while mechanically stimulated muscle tissue maintains a constant elastic modulus, indicating that mechanical stimulation is an integral aspect of maintaining tissue constructs for extended periods of time. Powell et al. also posited that mechanical stimulation might improve the penetration of culture media, a problem that remains an important aspect of creating and maintaining viable 3D tissue constructs *in vitro*.

Current techniques in mechanical stimulation of tissue-engineered skeletal muscle can be separated into two categories: passive unidirectional stretch and repetitive stretch. Passive stretch attempts to mimic the slow, passive tension found during bone growth. Repetitive stretch, or cyclic loading, attempts to mimic exercise by providing rapid, patterned uniaxial stretch. In several cases reported in the literature, both unidirectional stretch and repetitive stretch were accomplished *in vitro* using systems that relied on a computer-controlled stepper motor for precise stimulation via either slow incremental strain increases or rapid and repetitive stretch/relaxation cycles (Powell et al., 2002). Several different patterns of cyclic loading have been discussed in the literature. For example, Powell et al. exposed tissue constructs to five sets of stretch and relaxation within ten seconds, and then allowed the fiber to relax for thirty seconds. This was repeated in sets of three, followed by twenty-eight minutes of rest to complete a full cycle. This 30-minute cycle, shown in Figure 8 below, was performed at increasing strains (5% to 15%) over a period of eight days.

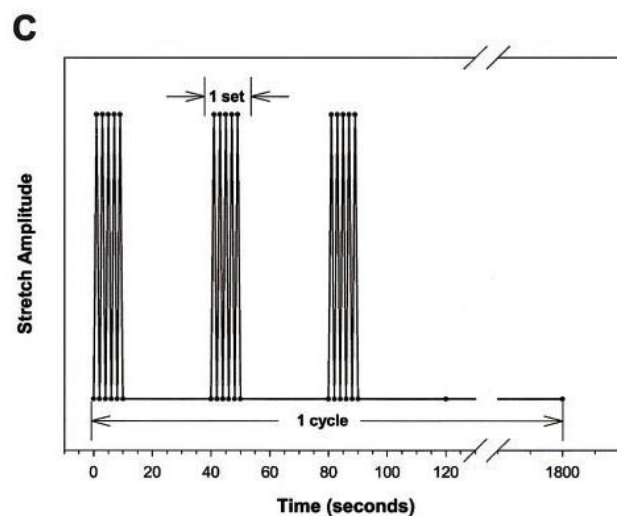


Figure 8: Cyclic Load Pattern (Powell et al, 2002)

Moon et al. instead stretched tissue constructs at 10% strain three times per minute for the first five minutes of every hour over periods ranging from five to twenty-one days. Both loading patterns, while very different, produced statistically significant muscle hypertrophy. As such, it is unclear how



specific load patterning affects the extent of muscle hypertrophy *in vitro*. Additionally, while these computer-controlled units accomplished consistent and highly defined mechanical stimulation, they also added to the cost and complexity of the tissue culture system, and similar results might be achievable with a simpler, more cost-effective means of stimulation, either via unidirectional stretch, repetitive stretch, or both.

While the benefits of mechanical stimulation have been widely discussed, there is still much to achieve before tissue-engineered skeletal muscle can approach the overall integrity and viability of native skeletal muscle tissue. While mechanically stimulated muscle tissue can exhibit up to ten-fold increase in myofiber diameter and contractile function compared to static culture, it still exhibits only about ten percent of the functionality of native skeletal muscle tissue (Moon et al., 2008). Although this disconnect in functionality may be caused by a whole host of interconnected factors, mechanical stimulation remains a significant issue, not only for the clinical promise of tissue-engineered skeletal muscle, but also for the study of tissue development and pathophysiology.

### *Innervation and Electrical Stimulation of TESM*

Another challenge in recreating the skeletal muscle natural environment is innervating the muscle or mimicking electrical stimulation. *In vivo*, deinnervated muscle atrophies to around 40% of the original innervated muscle (Powell et al., 2002). In a study conducted by Powell et al. they concluded that the small myofiber size in their results might have been due to a lack of innervation, assuming that the muscle was not receiving the appropriate growth factors and nutrients it would receive if it was innervated. Studies have shown that co-culturing muscle cells with neural cells or using transfected nerves has enhanced the contractibility and differentiation of TESM and created neuromuscular junctions (Bian et al., 2008). These neuromuscular junctions were acetylcholine sensitive and allowed for indirect stimulation of the muscle through the junction (Bian et al., 2002).

In a study conducted by Larkin et al. they co-cultured rat skeletal muscle tissue and spinal cord explants from fetal rats. The muscle cells were cultured using standard methods. When ready to differentiate, the muscle cells were seeded onto laminin coated culture plates. After two weeks the spinal cord extract was pinned into the muscle construct 12 mm apart, see Figure 9. One week later the monolayer was rolled up around the pin anchors. Sixteen days after being rolled into a cylindrical construct, the rolled monolayers were tested for contractile function. One of the pins was attached to a force transducer, and electrodes were placed on opposing pin anchors. Direct construct twitch stimulation was applied and contractile force was measured. Following this procedure a microelectrode

was attached to the neural extension to indirectly stimulate the muscle. Results showed that neural extensions stimulated only approximately 25% of the myofibers, compared to direct field stimulation. Addition of nerves showed no effect on muscle fiber diameter; however, maximum twitch increased from 40 to 100  $\mu$ N and maximum tetanus increased from 100 to 225  $\mu$ N for cultured muscle and cultured muscle with neural cells, respectively (Larkin et al., 2006).

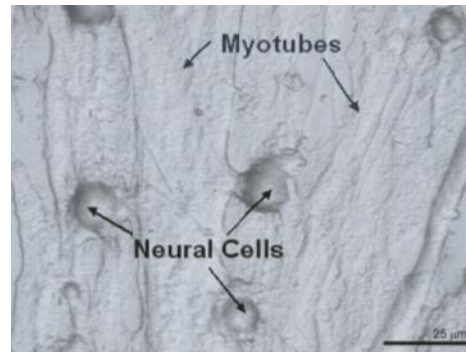


Figure 9: Light Microscopy of Neural Cells One Week After Plating (Larkin et al, 2006)

### 2.4.3: Producing Structural Integrity *In Vitro*

In order to achieve the desired level of stimulation to tissue-engineered skeletal muscle, the construct must have sufficient structural integrity. To achieve structural integrity, as well as provide a template for tissue growth, many solutions for creating tissue-engineered skeletal muscle involve the use of a scaffold or gel, onto which myogenic cells can be seeded. While there are many possibilities for the structure and composition of these constructs, all must meet some general requirements to be considered effective candidates. First, the scaffold must be able to support cellular proliferation and differentiation. It must be biodegradable, and should not exhibit toxicity during the degradation process. Finally, it should have mechanical properties that approximate those of native tissue as closely as possible (Liu, Ramanath, and Wang, 2008).

#### *Electrospun Fiber-based scaffolds*

Synthetic polymer fibers that degrade into non-toxic byproducts are viable options for producing effective scaffolds for tissue engineering applications. Polymer scaffolds produced by electrospinning have been shown to direct the migration of cells into aligned myofibers (Avis et al., 2010). Electrospinning is a process that allows for the creation of complex aligned microfibers onto which myogenic cells can be seeded for proliferation and differentiation (Liao and Zhou, 2009). These scaffolds are produced from biocompatible and biodegradable synthetic polymers such as PLGA and

PLLA. Despite the ability to produce well-aligned, striated myofibers, a disadvantage of this method is the reduced ability of cells to infiltrate the electrospun scaffold. Thus, cells attachment is mostly limited to the surface area of the scaffold construct (Avis et al., 2010).

### *Biological Cell/Gel Networks*

Biological gels are highly hydrated 3D structures made from materials such as collagen type I, collagen type IV, or fibrin. Since the materials for these scaffolds are either found in skeletal muscle ECM or part of a regenerative response to skeletal muscle injury, they are good candidates for tissue engineering and are capable of facilitating cell adhesion, proliferation, differentiation, and infiltration throughout the gel network (Drury and Mooney, 2003).

As a protein that is already found in the extracellular matrix of native skeletal muscle tissue, collagen is a good candidate for construction of 3D skeletal muscle tissue constructs. The architecture of collagen has been shown to allow for the alignment of myofibers, enabling a critical aspect of overall tissue functionality (Koning et al., 2009). Because of collagen's origin and role in skeletal muscle ECM, it is considered to be a good choice for enhancing skeletal muscle tissue regeneration.

Like collagen, fibrin can be used to form a 3D biological cell/gel network. In the case of fibrin, progenitor cells are mixed with a growth medium, fibrinogen, and thrombin to create a gel. After about 3 or 4 weeks, the cells can produce their own ECM proteins to replace the original fibrin matrix, achieving a fundamental goal of tissue engineering (Huang et al., 2005). Fibrin also has the ability to bind growth factors that enhance myogenesis (Koning et al., 2009).

Matrigel™ is a commercially available biological gel derived from Engelbreth-Holm-Swarm mouse sarcoma. Its main advantage is that it contains growth factors and ECM proteins. This gives Matrigel™ the special ability to modify gene expression and promote the rapid differentiation of progenitor cells into myoblasts, as well as the formation of myotubes (Kleinman & Martin, 2005). Despite its promise, Matrigel™ is both expensive and unsuitable for clinical use because of its cancerous and xenogeneic origin. However, Matrigel™ is still a viable scaffold option for experimental models, especially when combined with other biological gels, such as collagen or fibrin (Liao & Zhou, 2009).

### *Cell Sheets*

Currently, one of the major problems in using 3D scaffolds for tissue engineering in vitro is the difficulty of delivering culture medium to the center of the construct. As a result, cells at the center of a construct often become necrotic before or after mature tissue is formed (Drury and Mooney, 2003). One of the current methods being employed to work around this issue is the use of cell sheets. These are

very thin “2D” constructs, usually formed from various polymers or naturally derived substrates, to which media can easily be delivered. The sheets are then assembled into more robust 3D constructs after differentiation occurs (Koning et al., 2009). While this method is promising, the extra step of assembly adds a possible level of inconsistency and complexity to the tissue culture system. Additionally, the thickness of cell sheet constructs is limited by factors such as vascularization and blood supply.

### **Molding Systems**

Molding systems have also been used to produce a skeletal muscle tissue construct of a desired shape. In these cases a cell/gel network is usually cast into a mold, and the tissue is allowed to contract off of the sides of the mold as it forms, eventually producing a fiber-like construct. For example, Powell et al. used silicone molds with metal pins on either ends as attachment sites for the maturing tissue. These attachment sites were then actuated to provide mechanical stimulation to the tissue *in vitro* (Powell et al., 2002). Another system involved micropatterning of a silicone wafer, which was then coated with a substrate to promote primary rat skeletal muscle cell growth and adhesion (Das et al, 2009). This system, however, did not have defined attachment sites; therefore, it was not amenable to mechanical stimulation.

In 2011, a group of WPI undergraduate students designed a “dog-bone” shaped agarose mold to allow for the culture and anchoring of tissue-engineered skeletal muscle (Kalluri et al., 2011). The design incorporated agarose posts at either end of the mold to provide anchors for the maturing tissue. The system was able to form fiber like constructs with cells cast in collagen and fibrin networks, as well as self-assembled tissue. One of the drawbacks of this design was that the tissue construct was able to contract off of the anchoring posts (Kalluri et al, 2011). While the system was potentially amenable to mechanical stimulation, this was not achieved within the scope of the study.

## **2.5: Literature Review Summary**

This section presented an overview of skeletal muscle through a focus on embryonic development, muscle tissue components and structural hierarchy, and the mechanisms of healthy skeletal muscle tissue regeneration *in vivo*. The clinical motivations of acute muscle trauma and myopathies set the stage for a review of the current state of skeletal muscle tissue engineering. This discussion provides the necessary background for the following design strategy, which will attempt to

address some aspects of the multifaceted and complex problems present in the field of skeletal muscle tissue engineering.

### 3: Design Process and Strategy

In order to achieve this project's ultimate goal of designing a system that will model skeletal muscle tissue *in vitro*, we used the engineering design process (Dym and Little, 2009). The design process assisted us in analyzing the many considerations and factors that influence the creation of the final product. First, we reviewed the initial client statement and identified a list of objectives, constraints, functions, and means. Based on this list, we created a revised client statement to direct the conceptualization of design alternatives. These elements of the design process are discussed in the following chapter.

#### 3.1: Initial Client Statement

The following text represents the initial client statement given to our team, from which we identified the objectives, constraints, and functions that influenced our design alternatives.

"Currently, the laboratory uses extruded fibrin microthreads with human skeletal muscle derived cells seeded onto the surface and transplanted into SCID mouse skeletal muscle injury models to study the effect of various cell derivation and culture methods on functional tissue regeneration. The use of animals is time consuming and costly which severely limits the number of parameters that can be evaluated. Currently, the microthreads are produced first and then cells with myogenic potential are seeded onto the microthreads using a rotational cell seeding system. The limitations of this system include the ability to only achieve a cell density limited to the surface area of the microthreads and the system is not compatible with long term culture to evaluate the differentiation potential of the cells *in vitro*. For cylindrical tissue such as skeletal muscle fibers to form, the cells must degrade the microthread material and proliferate and migrate into the core. The proliferation phase of the cell cycle is not compatible with the quiescent phase required for cell fusion and matrix synthesis needed for skeletal muscle tissue formation. This could lead to premature breakdown of the tissue structure before the seeded cells can synthesize new matrix. An optimal situation would involve a system where cells could be seeded at the density required for cell fusion and tissue formation. However, the current microthread production process involves a stretching and drying step to produce axially aligned fibers, which is not compatible with seeding the cells within the microthreads at the time of formation.

A tissue engineered skeletal muscle system would enable the study of skeletal muscle tissue formation, maturation and the potentiality of cells entirely *in vitro* that could be used to approximate the utility of their use for the replacement of lost or damaged skeletal muscle tissue. The goal of this project is to design and produce a system that recapitulates skeletal muscle fiber structure into which myogenic cells can be seeded such that skeletal muscle tissue is formed. The system must be either produced aseptically or must be sterilizable and fit into an incubator in order to permit study of live cultures over time. The engineered system should further be amenable to the study of effect of mechanical strain and /or electrical stimulation on muscle fiber maturation and contractile function."

## 3.2: Objectives, Constraints, and Functions

According to the book “Engineering Design” (Dym and Little, 2009), objectives are statements about design characteristics that are desired by the client or end user, and are used to establish goals towards which effort is directed. Constraints are factors that limit the design, and if they are not satisfied the design is considered a failure. Functions are the actions that the design must be able to perform in order to achieve the objectives and meet the constraints through a set of means. The following sections describe each of these as they apply to our project.

### 3.2.1: Pruned Objectives

After identifying a large list of initial objectives from the client statement, we pruned this list and organized it into main and sub objectives. The list of pruned objectives can be seen below. Each of these objectives is a desired characteristic of the design as derived from the initial client statement.

- Should enable modeling of tissue formation *in vitro*
  - Timing of seeding for efficient cell cycle regulation
  - Support differentiation
  - Support proliferation
  - Approximate native tissue structure and directionality
  - Support tissue viability over time
  - Provide anchor for attachment of muscle tissue
- Should enable the study of skeletal muscle tissue
  - Formation
  - Maturation
  - Fiber density
  - Fiber strength
  - Fiber alignment
  - Contractile function
  - Influencing factors – other cells and cytokines
- Should be consistent/reproducible
  - Fiber length
  - Fiber diameter
  - Fiber strength
  - Fiber alignment
  - Contractile ability
  - Culture conditions
- Should allow for stimulation of produced muscle tissue
  - Mechanical stimulation
  - Electrical stimulation

From these pruned objectives, we constructed the pairwise comparison charts shown in Table 2-6 below. Pairwise comparison charts are used to rank objectives by comparing them to each other individually to determine which is more important. The objective that is deemed more important receives a score of 1, while the less important objectives receives a score of 0. Objectives that are tied in importance both receive a score of 0.5. Our client filled out these charts following this scoring system, which helped us to rank the objectives in order of importance to the client. These ranked objectives were used to make the future design decisions.

**Table 2: Main Objective Pairwise Comparison Chart**

Main Objective	1	2	3	4	Total Score	Rank
1. Should enable modeling of tissue formation	X	1	0.5	1	2.5	<b>1</b>
2. Should allow for stimulation of tissue	0	X	0	0	0	<b>4</b>
3. Should enable the study of tissue	0.5	1	X	1	2.5	<b>1</b>
4. Should be consistent/reproducible	0	1	0	X	1	<b>3</b>

**Table 3: Sub-Objectives of Objective 1 Pairwise Comparison Chart**

Sub-Objectives (Objective 1)	1	2	3	4	5	6	Total Score	Rank
1. Cell cycle	X	0	1	0	0	0	1	<b>5</b>
2. Support Differentiation	1	X	1	1	0	0.5	3.5	<b>3</b>
3. Support Proliferation	0	0	X	0	0	0	0	<b>0</b>
4. Approx. native tissue	1	0	1	X	0	0	2	<b>4</b>
5. Support viability	1	1	1	1	X	0.5	4.5	<b>1</b>
6. Provide anchor	1	0.5	1	1	0.5	X	4	<b>2</b>



Table 4: Sub-Objectives of Objective 2 Pairwise Comparison Chart

Sub-Objectives (Objective 2)	1	2	Total Score	Rank
1. Mechanical stimulation	X	1	1	<b>1</b>
2. Electrical stimulation	0	X	0	<b>2</b>

Table 5: Sub-Objectives of Objective 3 Pairwise Comparison Chart

Sub-Objectives (Objective 3)	1	2	3	4	5	6	Total Score	Rank
1. Formation	X	1	1	1	1	1	5	<b>1</b>
2. Fiber Density	0	X	0	0	0	1	1	<b>5</b>
3. Fiber Strength	0	1	X	0	0	1	2	<b>4</b>
4. Fiber Alignment	0	1	1	X	1	1	4	<b>2</b>
5. Contractile Function	0	1	1	0	X	1	3	<b>3</b>
6. Influencing Factors	0	0	0	0	0	X	0	<b>6</b>

Table 6: Sub-Objectives of Objective 4 Pairwise Comparison Chart

Sub-Objectives (Objective 4)	1	2	3	4	5	6	Total Score	Rank
1. Fiber length	X	0	0	0	0	0	0	<b>6</b>
2. Fiber diameter	1	X	0	0	0	0	1	<b>5</b>
3. Fiber strength	1	1	X	0	1	0	3	<b>4</b>
4. Fiber alignment	1	1	1	X	1	1	5	<b>1</b>
5. Contractile ability	1	1	0	0	X	1	3	<b>4</b>
6. Culture conditions	1	1	1	0	0	X	3	<b>4</b>

From these pairwise comparison charts, we determined that it is most important for our design to enable modeling of muscle tissue formation *in vitro*. In order to present the information from these tables, we constructed a weighted objective tree (Figure 10). The sub-objectives are listed below the appropriate main objective in order of their importance from top to bottom of the tree.

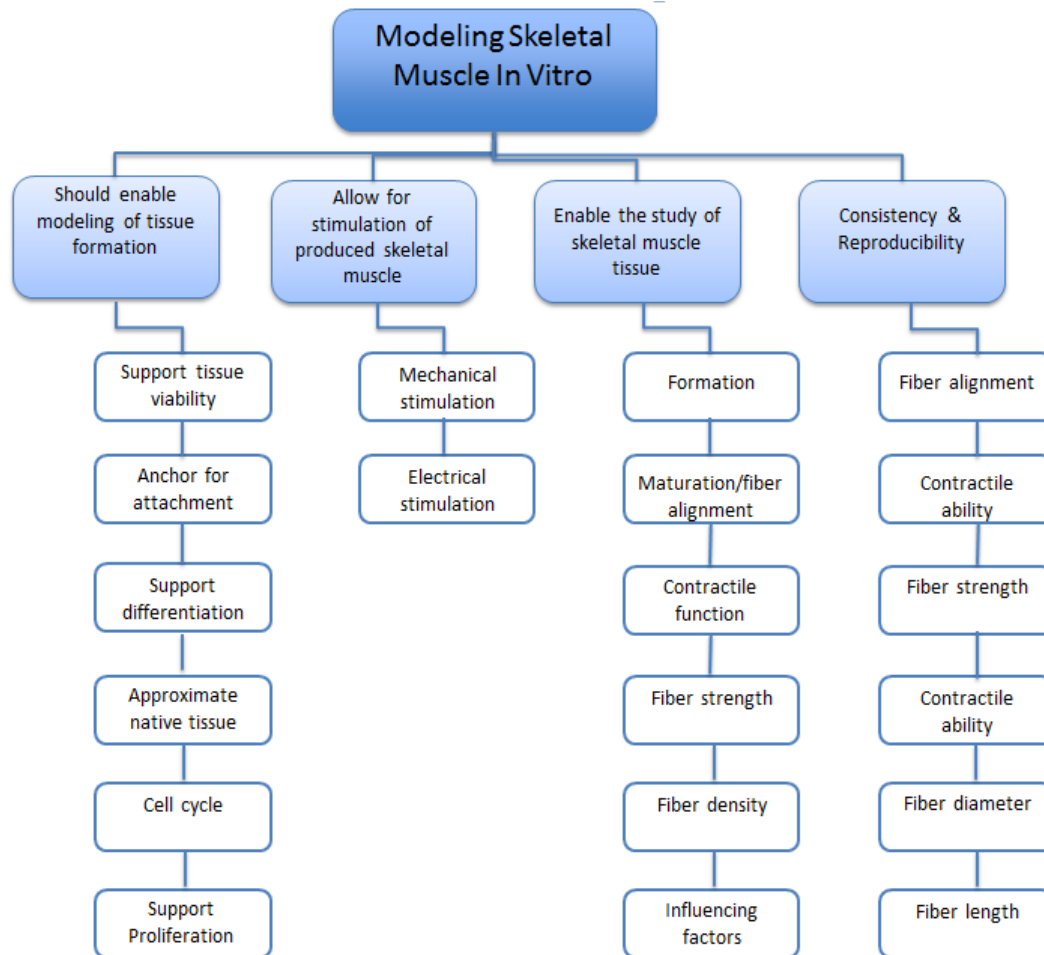


Figure 10: Weighted Objective Tree

### 3.2.2: Constraints

The constraints that we identified from the initial client statement are listed below.

- Must remain within budget
- Must operate within standard tissue culture environment
  - Fit in an incubator (no larger than 2' wide by 2' long by 1' high)
  - Mechanical parts, etc. must be able to function in high humidity (37°C, 5% CO<sub>2</sub>) environment

- Must be produced sterilely or be sterilizable
- Must be able to be prototyped and analyzed with biocompatible commercially available or easily accessible resources (i.e. on campus, collaborating labs, etc)
- Must be easy to use, safe, and time efficient

### 3.2.3: Functions

The functions that we identified from the initial client statement are listed below. These are the initial functions identified, which were pruned after the revised client statement was made to reflect the scope of the project. These revised functions can be found in the following chapter.

- Able to measure contractile function
- Able to anchor fibers to prevent tissue collapse
- Able to histologically and/or microscopically analyze resulting muscle tissue
- Able to adequately perfuse nutrients to tissue
- Able to electrically stimulate the tissue
- Able to support multiple cell types
- Able to mechanically stimulate the tissue
- Able to control environmental factors and physical components
- Able to support both proliferation and differentiation

### 3.3: Revised Client Statement

After identifying the above objectives, constraints, and functions, our team was able to distill the initial client statement down into a more concise and simplified statement of the team's overall purpose and main goals. This revised client statement was used to direct the rest of the project, starting with the conceptualization of design alternatives as described in the following chapter. The text of this revised client statement can be seen below.

"The purpose of this project is to design a method by which to consistently enable modeling of skeletal muscle tissue formation and function *in vitro*. This method should allow for anchoring of the produced tissue and would ideally be amenable to mechanical stimulation, electrical stimulation, and measurement of skeletal muscle tissue properties such as fiber density, fiber alignment, and contractibility."

## 4: Design Alternatives

After identifying the relevant objectives, constraints, and functions as discussed above, we brainstormed possible means to achieve each function and constructed a Function-Means Chart (Table 7 below). Constructing this chart was the part of the design process that allowed us to summarize the different possibilities for satisfying each individual function before we began to conceptualize initial design alternatives.

### 4.1: Needs and Functions Analysis

Based on the revised client statement, the team separated the functions into “needs” and “wants” based on what seemed feasible with the project’s available resources and time frame.

Needs: The following functions were identified as critical needs of the final design.

- Able to anchor fibers to prevent tissue collapse
- Able to mechanically stimulate the tissue
- Able to adequately perfuse nutrients to tissue
- Able to support both proliferation and differentiation

Wants: The following functions were identified as wants. These functions are less important to the design itself, but will still be considered in design decisions. For example, while the design itself may not include real-time measurement of contractile function, a separate method could be developed post tissue formation to assess this aspect of the design.

- Able to electrically stimulate the tissue
- Able to measure contractile function
- Able to provide support for cell growth through use of a scaffold

Table 7: Functions-Means Chart

Function	Means				
<i>Measure contractile function</i>	Force transducers at anchors - LabView	Spring scale			
<i>Anchor fibers</i>	Gel posts	Metal pins	Sutures	Angled posts/pins	Bowed post/pins
<i>Cell Proliferation/ Viability</i>	BrdU stain	Live/dead (nuclear stain)	Hoescht	MTT assay stain	H&E (hematoxylin and eosin)
<i>Cell Maturation/ Differentiation</i>	Myosin Heavy Chain	Sarcomeric $\alpha$ -actin, Myo-D, myogenin	CK (creatine phosphokinase activity)	FITC-phalloidine (actin)	Phase contrast imaging
<i>Perfuse nutrients (thickness)</i>	Mechanical stimulation	Constant media flow	Control fiber thickness	Cell sheets	Electro-spinning
<i>Electrically stimulate</i>	Jumper cables	Micro-electrodes	Stimulate neuron axon (in co-culture with neuronal cells)	Chemically (glutamate)	
<i>Scaffold to support cell growth and alignment</i>	Matrigel™	Collagen	Stamping with laminin	Extrude laminin microthread	
<i>Mechanically stimulate tissue</i>	Stepper motor	Balloon	Magnets	Screws	Cam

## 4.2: Alternative Designs

Design alternatives are useful for combining different means to achieve objectives in varying ways. This allows for different ideas to be explored and visualized when they might not otherwise have been realized. The feasibility of various components in these designs was evaluated in order to determine a preliminary design, which is presented later in the chapter. The sections below outline four design alternatives that the team created from the functions-means chart.

#### 4.2.1: Design Alternative #1

The first design alternative utilizes an agarose mold with a dog-bone shaped seeding channel similar to the most recent MQP design on this subject (Kalluri et al, 2011). One of the anticipated challenges that this design faced was that the skeletal muscle tissue would spontaneously contract out of the seeding channel or break near the agarose posts. Therefore, this design alternative takes advantage of this perceived challenge and includes an additional component directly above the agarose posts that will allow for the tissue to contract off the posts and out of the seeding channel onto metal pins. These pins would be bow-shaped to ensure that the tissue would not fall back down into the seeding channel once it contracts up onto the pins. These pins would then be actuated by a mechanism to provide mechanical stimulation, and potentially serve as a base for electrical stimulation later in the project. An initial sketch of this design alternative can be seen below in Figure 11.

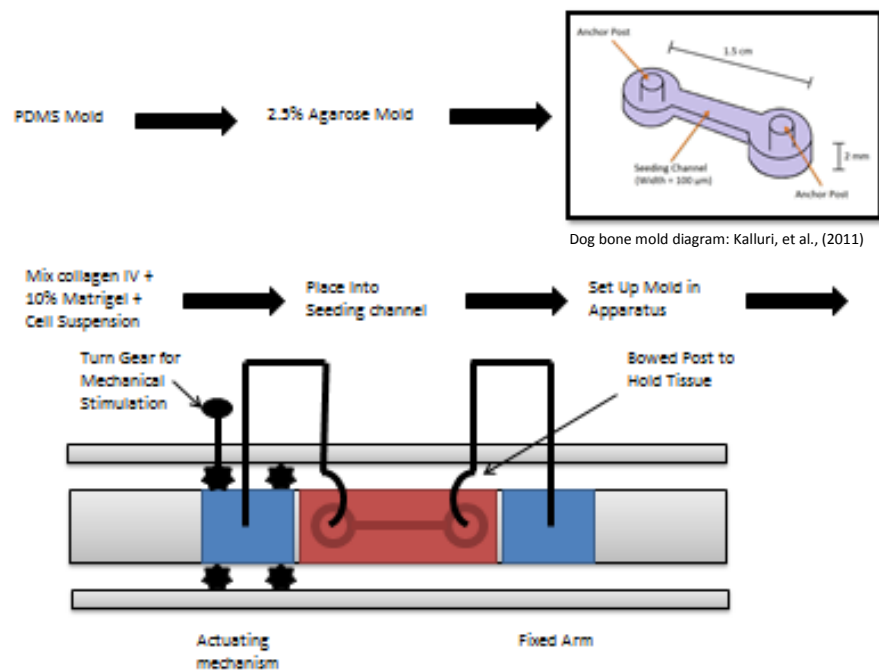


Figure 11: Design Alternative #1

#### 4.2.2: Design Alternative #2

The second design alternative is also based upon a previous MQP team's final design, but includes different modifications. This alternative integrates metal pins directly into the agarose posts, which would be used in much of the same manner for the tissue to contract out of the seeding channel. These pins would be anchored to the culture plate by cloning cylinders. One post would be rigidly fixed, while the other would be flexible. The flexibly anchored post would be moved back and forth by a magnet attached to a motor outside of the culture dish to produce cyclic loading on the tissue as it matures. Figure 12 below shows a basic CAD drawing of this design alternative. What is not seen in this picture is the agarose mold that sits in the base of the dish and surrounds the cloning cylinders. Also, the outside magnet that would be attached to the motor is not present but would be mounted to the right side of the dish to attract the magnetic pin.

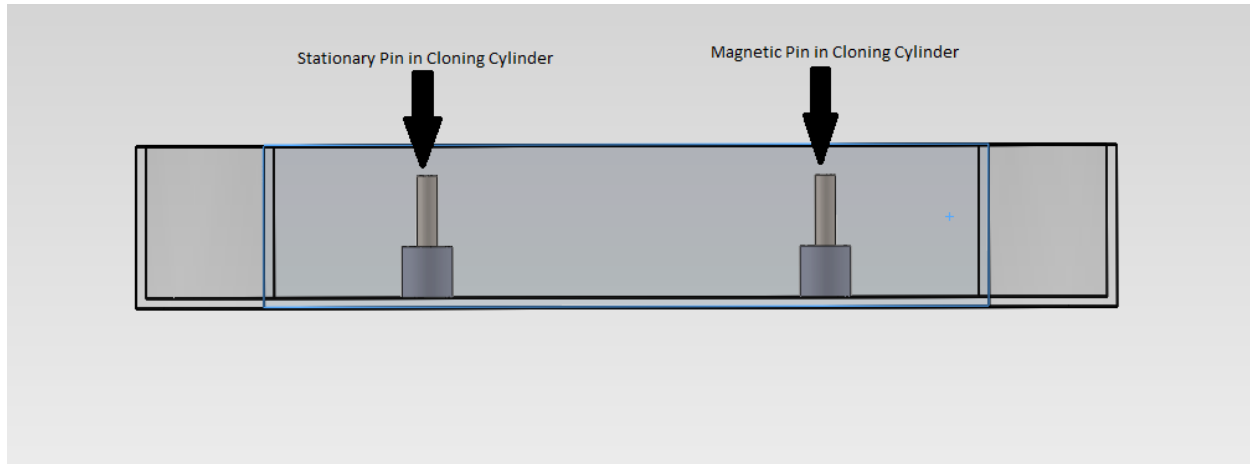


Figure 12: Design Alternative #2

### 4.2.3: Design Alternative #3

The third design alternative is inspired by Larkin et al.'s study (discussed in the Literature Review) and proposes culturing the C2C12 cells in a collagen sheet, and then rolling this cell sheet up around itself and allowing for further culture to produce a muscle fiber (Larkin et al., 2006). The ends of this rolled-up sheet could then be clamped to allow for mechanical stimulation. Electrical stimulation could be added in a later iteration of the design that would include laminin stamping as well as the collagen sheet to encourage neural cell growth and networking within the muscle tissue. An initial sketch of this design is shown in Figure 13 below, and represents a conceptual idea that the team did not pursue any further.

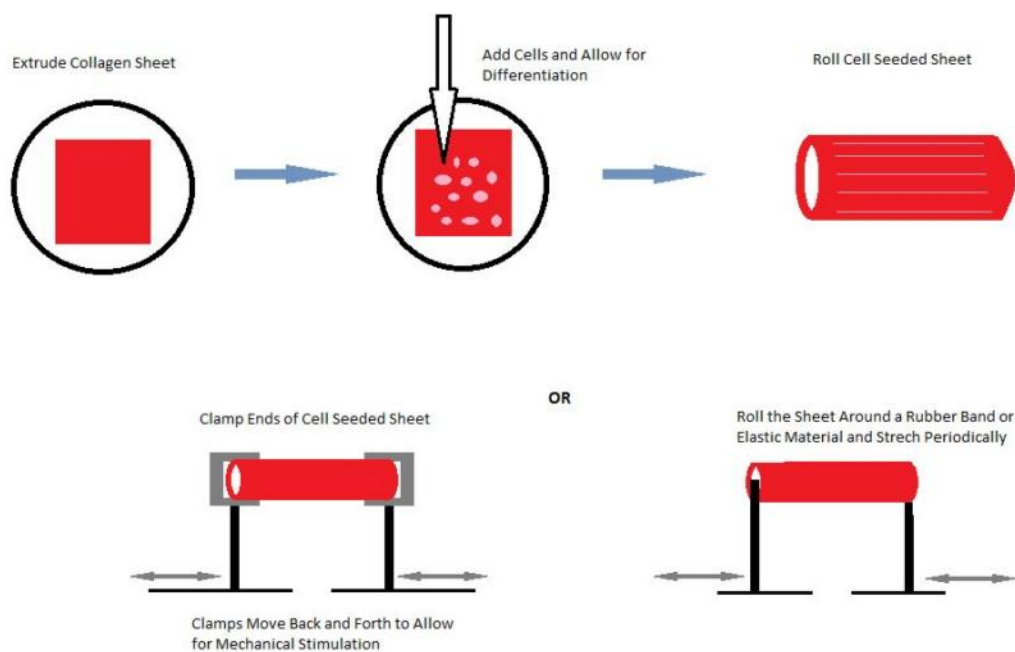


Figure 13: Design Alternative #3



#### 4.2.4: Design Alternative #4

The fourth design alternative returns to the original dog bone agarose mold and seeding channel, but replaces the agarose posts found at each end of the mold with metal posts. Once the cells have fused and formed multi-nucleated constructs that have anchored around the metal posts, the agarose mold will be cut away and a spring-loaded expander will be placed in between the tops of the two metal posts. This expander would be used to exert passive tension on the tissue. This design creates force pushing outward from between the posts, while the other design alternative focuses on pulling the posts from the outside. The SolidWorks drawing of this design alternative can be found below in Figure 14. It does not show the agarose mold in the bottom of the dish but rather just the pins that the tissue will ultimately form around as well as the spring apparatus that mounts to the tops of the pins.

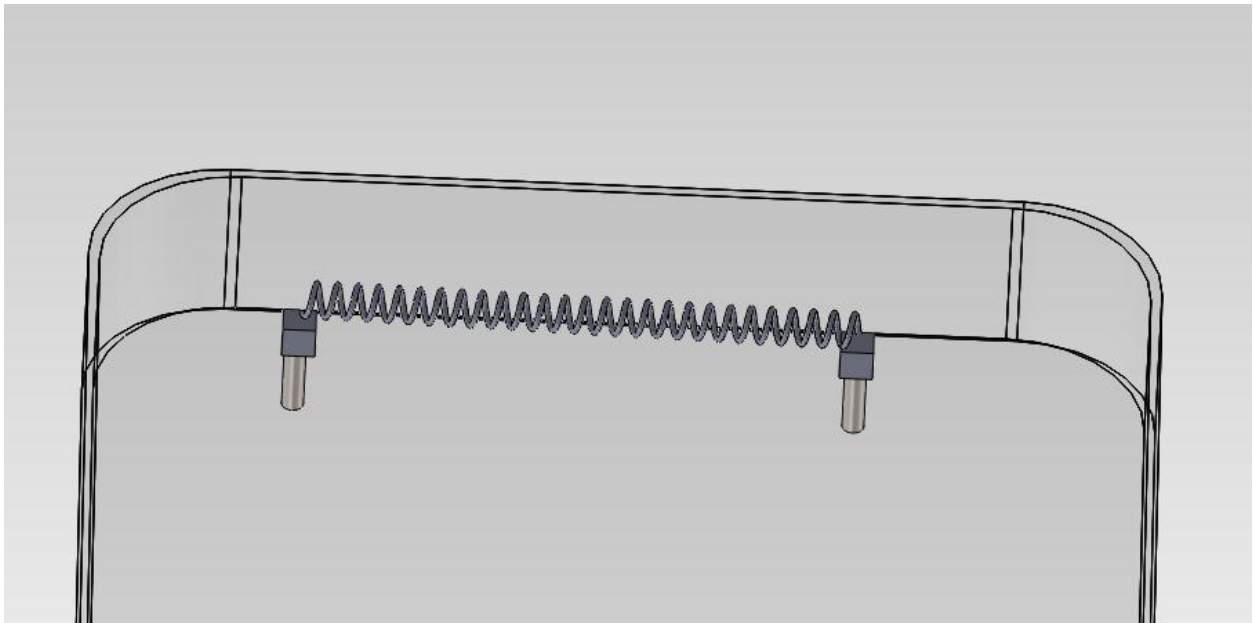


Figure 14: Design Alternative #4

### 4.3: Feasibility Studies

Before moving forward to select a preliminary design, it is necessary to evaluate the feasibility of various components and to determine the optimal cell culture environment for the design to function in. The components that were evaluated include the agarose molding process, the use of a magnet-driven mechanical stimulation method, and the maintenance and characterization of the C2C12 cells and their culture environment.

#### 4.3.1: Agarose Molding

The team decided to begin this design phase by testing the feasibility of using dog-bone molds for the final design. It was determined that it would be beneficial to study the effectiveness of several mold morphologies. First, a SolidWorks™ model was created in order to provide visualization of several mold types. This model is shown in Figure 15 below.

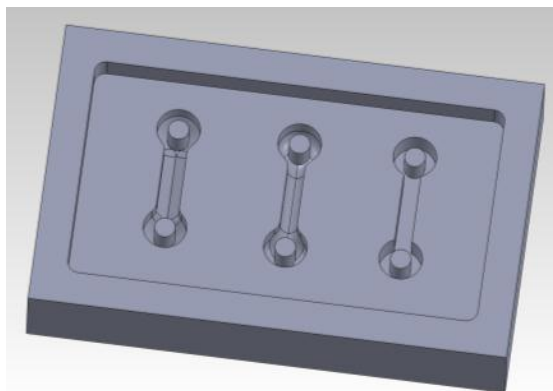


Figure 15: Mold Conceptualization

One mold features a V-shaped seeding channel, which would allow for scalable fiber sizes controlled by the cell number seeded in the bottom of the channel. The next mold has a U shaped bottom, and the final mold has a flat bottom, similar to the design created in a previous year's MQP.

While this model aided in mold conceptualization, the team realized that limitations in available machining and molding technology would not allow for sophisticated prototyping in a timely fashion. Since no data had been collected to justify the time necessary to create a sophisticated mold prototype, the team decided to develop a rapid prototyping technique to learn more. A positive mold was created using small, hollow tension pins attached to both ends of a 10 mm long piece of PVCA (polyvinyl chloride acetate). The PVCA was sanded down to a point and covered with aluminum foil in order to create a V-

shaped channel. The V shape was chosen for rapid prototyping as the team believed it had most promise for controlling tissue diameter.

### *Double-layer Casting*

A preliminary seeding channel was created in non-sterile conditions using the prototyped positive mold in agarose gel. Agarose powder was mixed with water in a designated concentration. The mixture was then boiled in a microwave to dissolve the powder. The solution was allowed to cool to approximately 60 °C before it was poured into a 60 mm tissue culture plate to height of 3 mm. Once this layer had gelled but not hardened completely, the positive mold was placed on top and another layer of liquid agarose was poured around the mold to a height of approximately 1 mm. The gel was allowed to set for 10 minutes before the mold was removed.

For the first two trials, a solution of 1% agarose was used. When the mold was removed, the agarose posts became lodged inside the tension pins and broke off from the culture plate. The seeding channel also collapsed partially, indicating that a higher concentration of agarose should be used to provide more structural integrity. For the next two trials, the concentration of agarose was increased to 2.5%. While this adjustment prevented the seeding channel from collapsing, the posts were still lodged inside of the tension pins, indicating that gel was extremely weak between the first and second gel layers. Figure 16 below shows one of the dog-bone channels with a missing post.



**Figure 16: Seeding Channel with Missing Post**

### *Single-Layer Suspension*

In an attempt to create a seeding channel with agarose posts intact, the team devised a method to suspend the positive mold in a single layer of agarose. This was accomplished by clamping the mold and suspending the clamp on a metal rod over the culture plate. When the correct height was achieved, a single layer of 2.5% agarose was poured into the plate until the mold was immersed in 1 mm of the solution. The gel was allowed to set for 15 minutes before the positive mold was removed.

The single layer suspension method resulted in a dog-bone shaped seeding channel that had intact posts extending about 3 mm above the bottom of the channel, as shown in Figure 17 below. While the team was able to create a rough prototype of an intact dog-bone seeding channel, the method of suspending the mold in a single layer of agarose was cumbersome and not ideal for the ultimate goal of creating seeding channels under completely sterile conditions. Thus, for the first sterile trials, the team decided to use the double-layer method, using the lack of agarose posts to test the feasibility of other anchoring materials.



**Figure 17: Seeding Channel with Post**

### *Sterile Mold Formation and Seeding*

To create a sterile molding system, a 2.5% solution of agarose in DMEM culture medium was autoclaved on a liquid cycle in a sterile bottle. The bottle was then transferred to a small incubator and kept at 60 °C to prevent the solution from solidifying. In the culture hood, the agarose-DMEM solution was pipetted into a sterile 60 mm culture plate to a height of about 3 mm. The positive mold was sterilized using a solution of 70% ethanol. After drying completely in the culture hood, the mold was placed on top of the first layer, and a second layer was pipetted around the mold to a height of about 1

mm. After 15 minutes, the mold was removed. As expected, the agarose posts broke off during mold-removal. The seeding channel was then covered in culture medium and allowed to sit in the incubator for two days. After this time, the culture plate was found to be free of contaminants. The medium was then aspirated from the mold and cells were seeded into the channel at a density of 2,500 cells/cm<sup>3</sup>. The cells were allowed to settle to the bottom of the channel for 10 minutes before another layer of new medium was added to cover the entire surface of the plate. One curved stainless steel suture needle was placed into the agarose in the center of the circular regions on both sides of the channel where the agarose posts had broken off. The mold was then placed inside the incubator overnight.

The next day, when the mold was examined under the microscope, the team discovered that all of the cells had balled up and died. Additionally, it was noted that a combination between low seeding density and imperfections caused by the rapid mold prototyping technique had prevented the cells from settling into a contiguous shape inside the seeding channel. The team noted that cells seeded as a control in commercially available Microtissue™ molds had also died. Since no contamination was visible in either the prototype mold or the control molds, the team guessed that a cytotoxicity issue may have caused the cells to die. The most important conclusion that the team learned from this experiment was the importance of having a uniform seeding channel to allow the cells to settle into a continuous formation, and that seeding density may also need to be increased to further address the need for a continuous tissue construct.

#### **4.3.2: Magnet Mechanical Stimulation Feasibility**

One of the team's most promising conceptual design ideas for the mechanical stimulation function was to use the attraction between two magnets to stretch the tissue construct in culture. Specifically, the team envisioned one magnet inside of culture, and one magnet outside of culture attached to an actuating mechanism. In order to test the feasibility of this idea, we rapidly prototyped a device that would allow us to gain data and determine if a magnet design would be possible.

Thin metal strips were taped down to a cardboard box to act as tracks. Next, metal sliders were attached to these tracks and nails were attached to both the tracks and the sliders. In doing this, the set of pins attached to the tracks would remain stationary and the other set would be able to move back and forth, stretching the tissue that would theoretically be wrapped around the pins. Finally, a magnet was attached across the two moving pins using hardening clay. The experimental setup is shown in Figure 18 below.

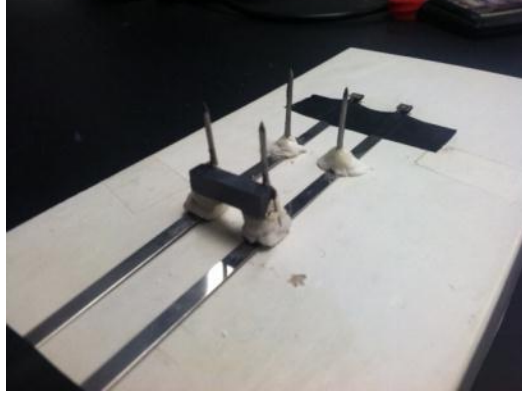


Figure 18: Magnetic Track-Slider Experimental Model

To test the feasibility of a magnetically actuated track-slider design, the free magnet was held at the same height as the magnet attached to the pins to ensure a perfect connection between the two. The free magnet was moved closer to the fixed magnet in one millimeter increments until the fixed magnet reacted and pulled the pins along the tracks to the free magnet. This process was repeated three times in order to obtain a precise measurement of the magnetic pull.

After three trials, we found that the magnets needed to be within 6 millimeters of each other before the fixed magnet moved toward the free magnet. The team then repeated this experiment with the addition of a culture dish wall placed between the magnets. Since we would ideally like our device to fit inside the cell culture dish, we needed to determine if the presence of the dish wall would affect the proximity necessary for magnetic attraction. With the dish placed 1 mm away from the inner magnet, the team gradually moved the outer magnet closer to the dish until the inner one was pulled towards the plastic wall. After three trials, the team discovered that magnetic attraction was experienced 4 mm away from the dish. Since the dish was approximately 1 mm thick, the team realized that the presence of the dish did not significantly affect the proximity necessary for magnetic attraction.

Our final experiment with the magnets consisted of putting 20 mm rubber bands around the pins to roughly simulate what would happen if there were actual tissue fibers stretched in the device. When the magnets became attracted to each other at 6mm apart, the rubber bands stretched before returning to their original positions once the outer magnet was moved out of reach. In each of three trials, the rubber bands stretched approximately 4 mm, to a strain of about 20%. Based on the results of these experiments, we decided that a magnetically actuated track-slider system could be feasible for the preliminary design.

## 4.4: Experimental Methods

The following section gives an overview of the cell culture techniques used in maintaining C2C12 cells, as well as a review of the experimental procedures associated with optimizing the culture of these cells for use in the device to model skeletal muscle tissue formation.

### 4.4.1: Cell Culture Maintenance

For the scope of this project, immortal myoblast C2C12 cells (available from the ATCC, Monasses, VA) were used to model skeletal muscle cells. These cells were maintained in DMEM/F12 culture medium supplemented with 10% fetal bovine serum (FBS), 2mM glutamax, and 1% penicillin/streptomycin, which supported their growth and proliferation. In order to avoid the spontaneous differentiation or loss of myogenic potential due to high cell density, the cells were passaged at subconfluence (50-70%) using 0.05% trypsin/EDTA in phosphate buffered saline (PBS). To passage the cells, the growth media was removed and the cells were washed two times with  $\text{Ca}^{++}/\text{Mg}^{++}$  free PBS to ensure that any molecules in the media that might inhibit the action of the trypsin were removed. The cells were then incubated with trypsin/EDTA at 37°C for 5 minutes, at which point most cells were detached from the surface of the culture vessel. The trypsin/EDTA was then neutralized through the addition of growth medium (to ensure the protease did not continue to degrade the cells after detachment was achieved), the cell solution was centrifuged at 1000rpm for 5 minutes, resuspended at a lower concentration in fresh growth medium, seeded into a new culture vessel, and returned to the incubator to allow undisturbed attachment. Cells were generally maintained in two T-75 flasks to ensure that there was a consistent and adequate supply of cells for experiments while maintaining a proliferative population.

C2C12 cells were induced to differentiate by replacing the growth medium with differentiation medium. This medium contained DMEM supplemented with 2% horse serum, 1% ITS (insulin, transferrin, sodium selenite), 1% penicillin/streptomycin, and 2mM glutamax. The drop in serum concentration as well as the change in serum type was the primary driving factor in inducing differentiation of the C2C12 cells. The differentiation process was generally completed by day 7 following the initial change from proliferation to differentiation media. Differentiation was considered complete when cells fused to form multi-nucleated myotubes, followed by the migration of the nuclei to the edge of the myotubes.

A number of standard cell culture calculations were used to characterize the proliferation and differentiation of the C2C12 cells. To characterize proliferation, the population doubling time (or the

time it takes for the number of cells in the culture vessel to double) was calculated using the following formulas:

$$PD = \log_2 \left( \frac{x}{x_0} \right) \quad \text{Equation 1}$$

$$T_d = \frac{PD}{t} \quad \text{Equation 2}$$

$T_d$  is the doubling time,  $PD$  is the population doubling,  $x$  is the final number of cells in the culture vessel,  $x_0$  is the initial number of cells in the same vessel, and  $t$  is the time between the initial and final cell counts. Cell counts were obtained using a hemocytometer and 10 $\mu$ L of resuspended cells obtained at the time of routine passaging. To characterize differentiation, the fusion index (or the percentage of cells that have differentiated and fused to become multi-nucleated myotubes) was calculated by dividing the number of nuclei that were found in fused myotubes by the number of total nuclei. The counts of these nuclei were performed using *ImageJ* software to mark and track nuclei.

#### 4.4.2: Optimizing Differentiation in Culture

A highly myogenic population of cells is needed in order to most effectively meet the design objectives and accurately model skeletal muscle *in vitro*. Though following the standard differentiation protocol for C2C12 cells as previously described can consistently yield a reasonable amount of fully differentiated cells, optimizing the differentiation process will ensure that the highest percentage of C2C12 cells differentiate. Specifically, the seeding time and density of cells into the device, as well as the purity of the cell population and serum levels in the differentiation medium, can affect the level of differentiation of C2C12 cells. Experiments to evaluate the effect of each of these factors were performed to determine the ideal combination of factors that will yield the highest percentage of successfully differentiated C2C12 cells.

##### *Seeding Density*

Optimizing the seeding density of differentiating cells into the device is important in order to produce the healthiest differentiation of skeletal muscle tissue. If the cells are seeded too sparsely into the device, they will not be able to attach to one another and fuse to form myotubes, and will die. However, if the cells are seeded too densely, they could overgrow the device in an unaligned mass of myotubes. In order to evaluate the effect of different seeding densities, C2C12 cells were first seeded into a 24-well plate at varying concentrations per well, as shown in Figure 19 below.



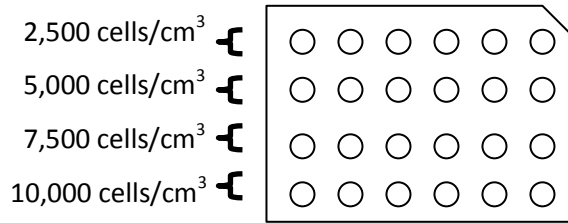


**Figure 19: Seeding Density Experiment Schematic**

We then maintained the cells in the plate until the most highly concentrated wells reached confluence, at which point we began the differentiation protocol previously described. At Day 7 after differentiation was induced, the entire 24-well plate was fixed by removing the medium, washing twice with PBS containing calcium and magnesium, incubating for 10 minutes with ice cold methanol, and then washing again with PBS. All wells were then stained with anti-myosin and conjugated with fluorescent probes (AlexaFluor-488, Invitrogen) to identify the differentiated cells, followed by counterstaining with Hoechst to identify whether or not the nuclei had fused. Each well was incubated with a blocking solution for 30 minutes at room temperature, then the blocking solution was aspirated and the wells were incubated in anti-myosin primary antibody diluted 1:500 in PBS/0.05% tween solution for an additional 30 minutes. The wells were then washed four times with PBS for 3 minutes each wash, and then incubated with a fluorescent probe conjugated with the secondary antibody (Alexafluor-488) for 30 minutes while protected from light. The wells were washed another 4 times with PBS, and then Hoechst dye was added at a concentration of 0.5µg/mL in PBS. The cells were then imaged with a fluorescent microscope, and analyzed for nuclear fusion as previously described. The cells were also analyzed for myosin expression (which appeared as green fluorescence) and location of nuclei (which appeared as blue fluorescence), to determine which cells had differentiated and were expressing myosin in addition to being multi-nucleated, both of which are marks of successful differentiation.

### ***Timing for Seeding Molds***

The timing of seeding cells into the device can also have a significant effect on the level of differentiation achieved. If the cells are seeded too early in the process of differentiation, when not enough of the cells have exited the cell cycle, the cells that are still proliferating can compromise the integrity of the tissue by not producing enough extracellular matrix material. However, if the cells are seeded too late in differentiation, the population of cells that have exited the cell cycle will be too large, and not enough proliferating cells will be left to fill the device before they also begin differentiating. To determine the optimal time in the differentiation process that would provide a balance between

proliferating and differentiating cells, two 12-well plates were seeded with 2,500 cells/cm<sup>3</sup>, and differentiation was induced as previously described when the cells were approximately 70% confluent. Starting at Day 2 after inducing differentiation, a row of 3 wells was incubated with BrdU at 1μl per mL of growth media. BrdU is a thymidine analog that is incorporated into the DNA of replicating cells, and can be detected using immunofluorescence. After 8 hours of incubation with BrdU, the 3 wells were fixed using methanol as previously described. This process was repeated for different rows for Days 3-7 of differentiation, at which point all wells had been incubated with BrdU and fixed in methanol. The wells were then incubated in 1.5 N HCl at room temperature for 20 min. The wells were then incubated in blocking serum for 15 minutes, after which the blocking serum was replaced with anti-BrdU primary antibody diluted 1:500 in PBS/0.05% tween for 30 minutes. Each well was then washed three times with PBS for five minutes each wash. A fluorescent probe conjugated with the secondary antibody was diluted 1:500 in PBS/0.05% tween. This solution was then added to each well, and allowed to incubate for 30 minutes while protected from light. The wells were washed another 4 times with PBS, and then Hoechst dye was added at a concentration of 0.5μg/mL in PBS. The cells were then imaged with a fluorescent microscope. Nuclei of all cells appeared blue, while only the nuclei of proliferating cells appeared green, which allowed for analysis of the levels of proliferating cells compared to total cells at each day during differentiation.

### *Serum Concentration*

Serum concentration in the differentiation medium is another factor that can affect the level of differentiation observed in C2C12 cultures. To observe the levels of proliferative vs. differentiating cells in differentiation media containing varying levels of serum, C2C12 cells were plated at 2,500 cells/cm<sup>3</sup> in 20 wells of a 24-well plate. These cells were maintained until they reached approximately 70% confluence, at which point differentiation was induced as previously described with 2% horse serum in the media. At Day 3 after differentiation was induced, a row of 5 wells was incubated with BrdU for 6 hours and fixed with methanol as previously described. At Day 4, another 5 wells were incubated with BrdU and fixed before the media was changed on the remaining 15 wells. At this media change, wells received differentiation media containing varying levels of serum: 2 wells received media with normal 2% serum, 2 wells with 1.5% serum, 2 wells with 1.0% serum, 2 wells with 0.5% serum, and 2 wells with 0% serum. For Days 5 and 6, one of each of these wells was incubated with BrdU and then fixed with methanol. These wells were then stained with anti-BrdU, Alexfluor-488, and Hoechst as previously described and imaged with a fluorescent microscope. This experimental design collected data for the

two days before and after the media change containing varying levels of serum, allowing the evaluation of the effects of the change in serum levels on the levels of differentiating vs. proliferative cells. Staining with BrdU enabled the evaluation of the levels of proliferating cells, while counterstaining with Hoechst allowed the observation of the number of cells that had exited the cell cycle (the nuclei of these cells appeared blue, with no green indicative of the presence of BrdU).

### **Purification**

An alternative strategy to increasing the myogenic potential of the cell population is purification through pre-plating, similar to described protocols for isolating embryonic stem cells. A population that has been purified to contain almost exclusively myogenic cells will have a higher percentage of differentiation than a population that has not been purified. In this experiment, 500,000 proliferating C2C12 cells were plated onto a T-75 flask and allowed to adhere for 5 minutes, at which point the media and remaining cells in suspension were transferred to a new flask and the media was replaced in the old flask. This process was repeated every five minutes until evidence of quickly adhering cells as observed by microscopy decreased. This resulted in four flasks with four different populations of cells that adhered at four time points, each 5 minutes apart. The cells in these flasks were allowed to adhere and proliferate for an additional 24 hours, at which point cells from each flask were plated at 5,000 cells/well on 4 separate 4-well plates. The remaining cells were passaged into separate flasks to maintain the isolated populations. When the cells in the 4-well plates reached approximately 70% confluence, differentiation was induced as previously described. At Day 7 after differentiation was induced, all wells were incubated with BrdU for 6 hours and then fixed with methanol. The cells were then stained for myosin and BrdU, counterstained with Hoechst, and imaged using a fluorescent microscope. This experiment allowed the determination of the difference in myogenic potential between populations, as well as the levels of proliferative cells present in each population. The percent of proliferating cells dropped as the number of platings increased, and the last plating represented a highly myogenic population of mainly differentiated cells that expressed myosin, fused into continuous myotubes, and showed relocation of nuclei to the edge of the myotubes. This population of cells was grown up in and used for the rest of the project.

### **4.4.3: Optimizing Tissue Construct Formation**

Translating the culture of C2C12 cells from 2-dimensional sheets to 3-dimensional tissue constructs required additional optimization, especially in the area of seeding density. To determine which seeding density produced appropriate tissue constructs, two rounds of experiments with

incrementally increasing seeding densities were performed. C2C12 cells were grown and differentiated as previously described, and seeded into ring-shaped agarose molds (with an inner post diameter of 2 mm) 48 hours after differentiation was induced. Seeding densities ranged from 5,000 cells/ring to 2,000,000 cells/ring, and the total number of cells was consistently seeded in 100 $\mu$ L of differentiation medium. The molds were checked 24 hours post-seeding for macroscopic and microscopic evidence of tissue formation. If tissue had formed and was intact, additional differentiation medium was gently added to the mold to fill the well and cover the tissue. Tissue constructs were observed daily and differentiation medium was added as needed to keep the tissue and the agarose hydrated.

Tissue rings that formed from different seeding densities were then fixed at varying time points for histological evaluation. Histological sectioning is an experimental method that can be used to observe the structural anatomy of the cells within tissue sections. Tissue samples are fixed, processed, embedded, sectioned and then stained. The methods for tissue processing and staining are discussed below.

### *Tissue Processing*

When a sample is ready for histological processing, the tissue can be fixed using 4% formaldehyde. First, remaining medium was aspirated from the sample, followed by a PBS rinse. Then, the sample was immersed in 4% formalin for approximately 30 minutes. If the sample was not to be processed immediately, formalin was aspirated from the sample, which was kept hydrated in phosphate buffered saline at 4°C.

When ready to process, the samples were placed in appropriate-sized cassettes with informational labels. Samples then went through a dehydration process. This process began with a 15-minute incubation in 70% ethanol, followed by incubations in 80%, 95%, and 100% ethanol. The dehydration process ended in two subsequent immersions in xylene for 30 minutes and two paraffin incubations for 30 minutes.

After the second paraffin incubation, the samples were ready to be embedded. Samples were taken to an embedding station in which the tissue sample was placed in a small dish and immersed in wax. Application to a cold surface embedded the tissue in a wax block. The slow solidification of paraffin wax allowed for the user to embed tissue at the desired angle for sectioning.

A microtome was used for the embedding process. Tissue sections were cut at approximately 4  $\mu$ m thickness. For cleaner sections, wax blocks were placed on ice before sectioning and extra wax

trimmed from around the tissue. Following tissue sectioning, slices were placed in a warm water bath and then mounted on charged slides.

### *Hematoxylin and Eosin Stain*

Hematoxylin and Eosin (H&E) is a commonly used stain in histological sections. The hematoxylin stains the nuclei of cells blue and eosin counterstains the cytoplasm pink. This stain is used to view the basic structure of the tissue.

To prepare the samples, wax was baked off the slides for approximately 1-2 hours. Then, the slides were rehydrated by incubation with decreasing dilutions of ethanol (100-70%). Nuclei were then stained with hematoxylin and then the sample were washed with running water. Samples were then dipped in 0.3% acidic alcohol and rinsed with tap water. The samples were counterstained with Eosin, rinsed with water, and then dehydrated in increasing concentrations of ethanol. Samples were then ready to be mounted with a clear cover slip and imaged.

### *Myosin Stain*

Myosin staining in immunohistochemistry is used to observe the presence of myosin and allow for the calculation of the fusion index. For the purposes of our experiments, a DAB Impress Kit from Vector Labs was used for myosin stain antibodies. Samples followed the same baking and rehydration process described in the H&E staining methods. Vector antigen unmasking solution was added to approximately one liter of water and placed in a pressure cooker. Slides were placed in the pressure cooker once the solution begins to boil and cooked for 20 minutes. Following unmasking, slides were rinsed with water and PBS, and then incubated with 2.5% horse serum. Samples were then washed with PBS three times and incubated with primary antibody dilution. After 30 minutes, the samples were washed with PBS three times and incubated with H<sub>2</sub>O<sub>2</sub>. After washing with PBS, anti-mouse IgG was applied followed by another wash with PBS. Then Impact DAB substrate was applied until desired color was observed. The reaction was stopped with a tap water rinse and mounted to a cover slip.

## **4.5: Preliminary Data**

The following section gives an overview of the results obtained from the experiments described above. These results were used to ensure that the cell culture environment of the C2C12 cells in the device is optimized.

#### 4.5.1: Optimizing Differentiation in Culture

The seeding time and density of cells into the device, as well as the purity of the cell population and serum levels in the differentiation medium, can affect the level of differentiation of C2C12 cells. Experiments to evaluate the effect of each of these factors were performed to determine the ideal combination of factors that will yield the highest percentage of successfully differentiated C2C12 cells, the results of which are discussed below.

##### *Characterizing Proliferation Rate*

As cells were maintained and grown in culture, cell number was recorded at the time of each subculture. Using Equation 1, population doublings, and Equation 2, doubling time, the team was able to calculate the number of population doublings that occurred between plating and subculture. Figure 20 below shows the data used to deduce the population doubling rate.

$$\begin{aligned}x &= 710,000 \frac{\text{cells}}{\text{mL}} * 10\text{mL} = 7,100,000 \text{ cells} \\x_0 &= (867,500 \frac{\text{cells}}{\text{mL}} * 10\text{mL})/10 = 867,500 \text{ cells} \\t &= 48 \text{ hours} \\PD &= \log_2 \left( \frac{7,100,000}{867,500} \right) = 3.032883 \text{ PD} \\t_d &= \frac{3.032883 \text{ PD}}{48 \text{ hrs}} = .063185 \frac{\text{PD}}{\text{hrs}} * 24 \text{ hrs} = 1.51644 \text{ PD/day}\end{aligned}$$

Figure 20: Population Doubling Time Calculations

From this information, the population doubling time was defined as approximately 1.5 population doublings per day, or 1 population doubling every 16 hours. This information is valuable in estimating the timing of future experiments, and has been used since to maintain a healthy C2C12 culture as well as plan for and set up effective experiments.

##### *Seeding Density*

Cells plated at four different cell seeding densities (2,500 cells/cm<sup>3</sup>, 5,000 cells/cm<sup>3</sup>, 7,500 cells/cm<sup>3</sup>, 10,000 cells/cm<sup>3</sup>) were allowed to proliferate for two days post plating. On day 0 differentiation medium was added and images were taken using a Zeiss microscope at 20x

magnification. Six days later plates were stained with anti-myosin and Hoescht. Figure 21 below shows the fluorescent images from this experiment with the confluency at which differentiation was induced as evidence by phase contrast microscopy.

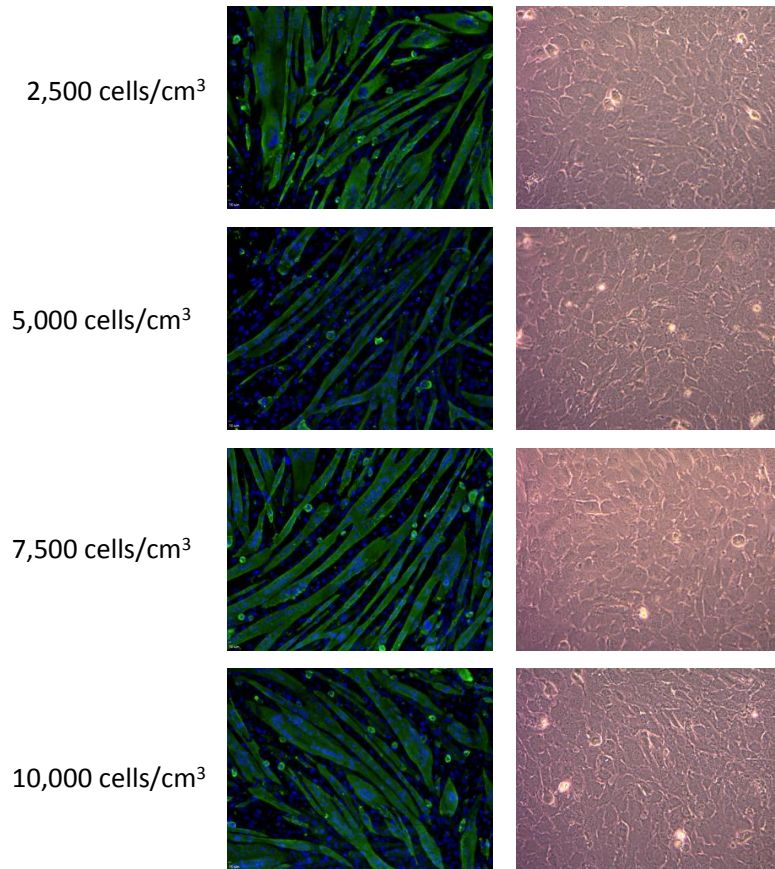


**Figure 21: Seeding Density Images**

*Differentiation to myotubes with different cell seeding densities. (left) Cell seeding density per unit area. (middle) Myosin staining (green) with Hoescht (blue) on day 6 (right) Phase contrast microscopy using Ziess microscope at 20x magnification on day 0.*

Fluorescent imaging shows that differentiation was successful at all four seeding densities. Fibers appear to be more densely packed at 7,500 cells/cm<sup>3</sup> and 10,000 cells/cm<sup>3</sup>. To further analyze these images, the fusion index was calculated using one representative image from each seeding density. Figure 22 below illustrates the fusion indexes of different seeding densities.

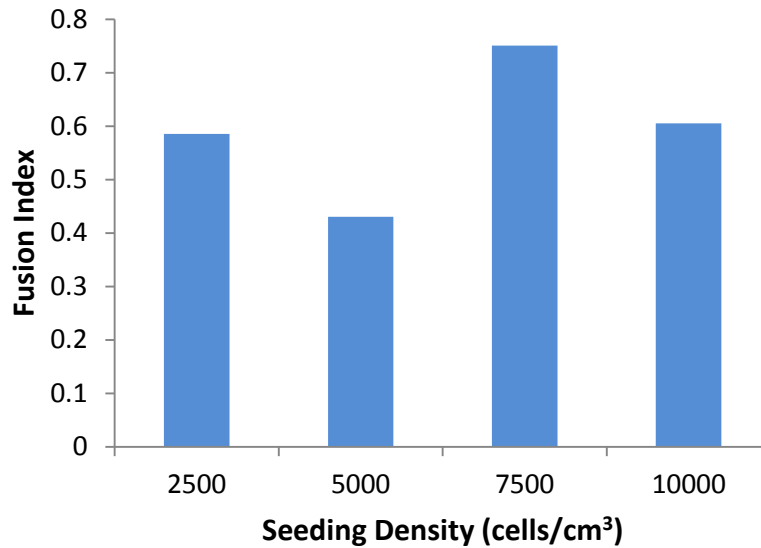


**Figure 22: Fusion Index vs. Seeding Density**

*ImageJ analysis of fluorescent images to calculate the fusion index for each seeding density.*

Fusion index calculations indicate that in order to achieve maximal fusion or differentiation the best cell seeding density is 7,500 cells/cm<sup>3</sup>. This cell seeding density will be used in future experiments to ensure the most effective differentiation of cells into mature skeletal muscle tissue.

### ***Seeding Timing***

Cells plated at a uniform density were examined from at two to seven days after differentiation is initiated. Prior to fixation cells were incubated with BrdU in order to calculate the number of cells still in proliferation versus the number of cells that have differentiated. The plates were imaged with a fluorescent microscope, shown in Figure 23 below. Also seen in Figure 23 is the *ImageJ* analysis of these images.



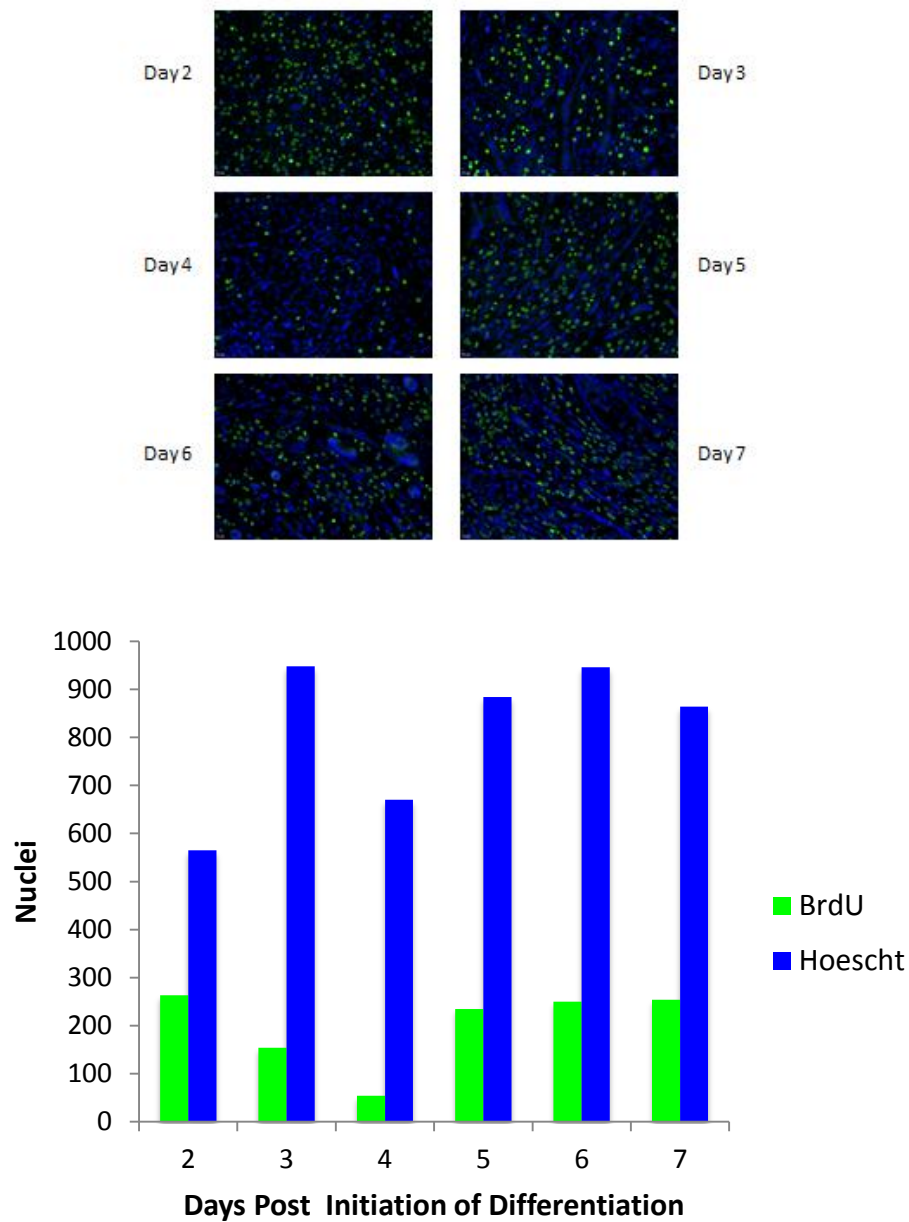


**Figure 23: Seeding Timing Images and Nuclei Count**

*(Top) Day 2-7 post addition of differentiation media, C2C12 cells stained with BrdU (green) and Hoescht (Blue)*

*(Bottom) Quantification of nuclei stained using ImageJ*

Days 2-3 show a marked decrease in the number of cells in proliferation. However at Day 4, the images showed a noticeable increase in BrdU-stained cells, which indicates an increase in the amount of proliferative cells in our population. In reviewing our lab notes, we noticed that Day 4 was the day we performed a media change. This could indicate that our cell population is not composed entirely of

myogenic cells with the potential to differentiate, but that it may also include a number of fibroblastic cells that showed a proliferative burst when the media was replaced and they received an influx of serum. The data presented above indicates a need for purification of the cell population or the use of a lower serum concentration in differentiation media to lower the proliferative burst, both of which have the potential to optimize the differentiation and myogenic potential of the C2C12 population that we are working with.

#### 4.5.2: Optimizing Tissue Construct Formation

Through seeding partially differentiated C2C12 cells at varying densities, a minimum seeding density of approximately 233,000 cells/ring was identified as necessary for the formation of continuous tissue. Any seeding densities less than this produced tissue that broke after formation, shown in Figure 24 below. These low seeding densities also resulted in the lack of tissue formation.

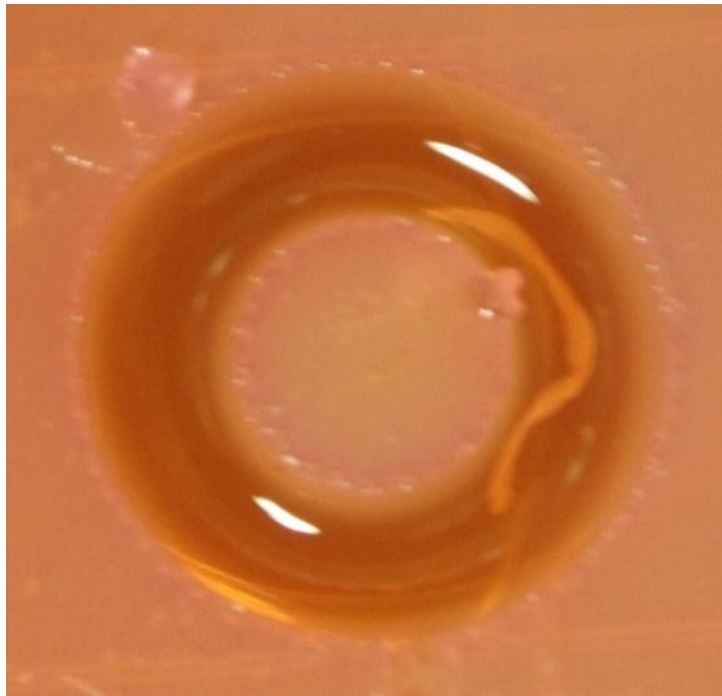


**Figure 24: Ring broken after tissue formation**

A maximum seeding density of 500,000 cells/ring was also identified, as any tissue produced above this density was too large in diameter to support adequate nutrient diffusion. Figure 25 below shows images from the histological sectioning and H&E staining of rings at the minimum (left) and maximum (right) seeding densities. The tissue formed with 233,000 cells/ring showed superior concentric cellular and nuclear alignment. Less alignment was observed in the tissue formed with

500,000 cells/ring, but this thicker tissue contained areas of more advanced differentiation, as shown by the boxed multi-nucleated myofiber. Because the thicker tissue was also easier to handle and less prone to breaking, a seeding density of 500,00 cells/ring (or 5,000,000 cells/cm<sup>3</sup> of mold volume) was used for the duration of the project.

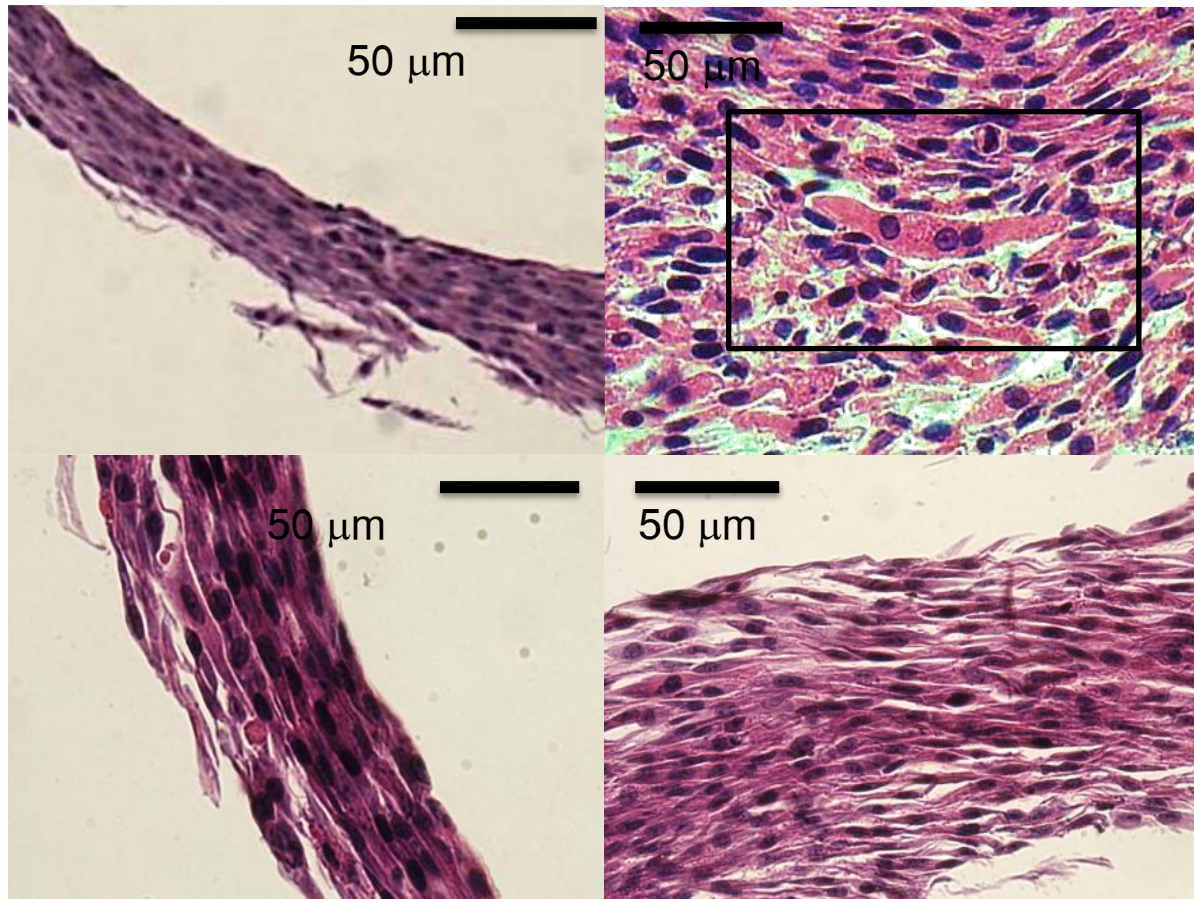


Figure 25: H&E Staining of C2C12 Tissue Constructs  
(left) Thin Rings: 233,000 cells/ring, 5 days post-seeding (right) Thick Rings: 500,000 cells/ring, 2 days post-seeding

## 4.6: Preliminary Design

Based on the preceding feasibility studies and experiments, the team arrived at a complete preliminary design for the sustained culture and mechanical stimulation of tissue-engineered skeletal muscle.

### 4.6.1: Molding System

After learning from the experiences with the rapid-prototype mold, the team decided that a more uniform mold was necessary to create functional seeding channels. The team also determined that the mold should be autoclaveable, in order to avoid any possible contamination. Additionally, a system created through machining and PDMS casting imposed undesirable limitations on mold dimensions. Thus, the team arrived at a compromise between inaccurate rapid prototyping and more involved manufacture using machining and PDMS casting. This compromise made use of casting wax and a commercially available, self-curing, thin-pour polymer called Reprorubber™. Reprorubber™ is both non-cytotoxic and autoclaveable once it has set, and unlike PDMS, it does not require a heating cycle to cure. This factor enables the use of casting wax, which has a low melting point. With this system, a precise and uniform negative mold can be pressed into the casting wax. Reprorubber™ can then be poured over the negative to create the positive mold, which can easily be removed and trimmed using a razor blade once it has set at room temperature. The positive mold created through this method will create four parallel 10mm long by 1mm deep V-shaped seeding channels with 1mm deep, 4 mm diameter circular depressions on either end to allow for the implantation of stainless steel anchoring points.

### 4.6.2: Culture Vessel and Mechanical Stimulation Device

The molding system described above is compatible with the combination culture vessel and mechanical stimulation device shown in Figure 26 below. Letter A shows a commercially available square tissue culture dish, in which the majority of the device is constructed. Letter B shows one of two tracks fixed to the top of the culture dish, in which component C can slide back and forth. Letter D shows a base, which functions to keep the culture dish stationary and allows for the attachment of a motor.

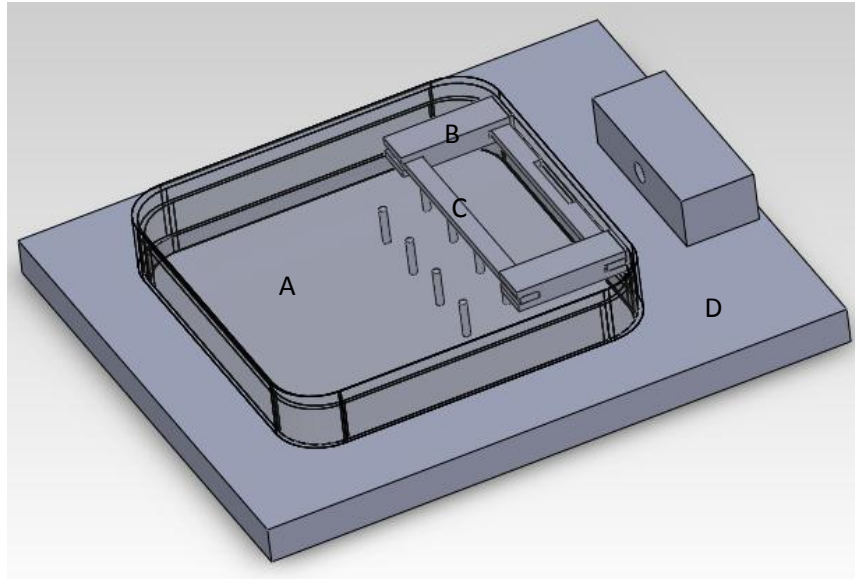


Figure 26: SolidWorks™ drawing of preliminary design for mechanical stimulation

A layer of agarose is cast in the bottom of the culture plate and allowed to set around four anchoring pins. Another layer of agarose is poured and the positive mold is immediately placed over the pins so that the opposite end of the mold is precisely aligned with the pins included in the component labeled C. Once the gel has set, the mold is removed to create the seeding channels. The channels are then seeded at a high density, and the culture dish lid, which contains components B and C, is placed on top so that the pins slightly penetrate the agarose in the end of the seeding channel opposite the fixed pins. Each of the components and their functions are described in greater detail in the section below.

### ***Component A- Culture Dish***

The team selected 100mm x 100mm x 15mm square culture dish for use in the design. A square dish was selected to ensure that the magnets used to actuate the tissue are parallel to the edge of the culture dish. This enables the magnets to be placed close enough to each other to facilitate attraction. The curved edge of a circular culture dish would cause the magnets to be located farther apart, which would make designing the actuating device more difficult. Four pins are attached to the bottom of the culture dish as shown in Figure 27 below. These pins provide a fixed attachment point for the muscle tissue and will also serve as a guide for the location of the molding system to be used in conjunction with the device.

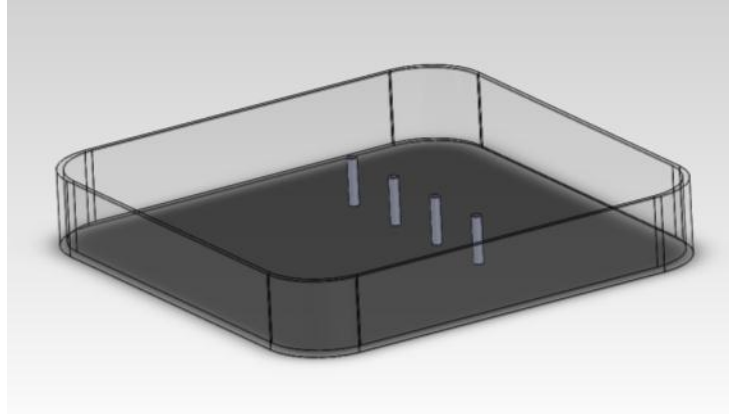


Figure 27: Bottom of Culture Dish

### *Component B- Tracks*

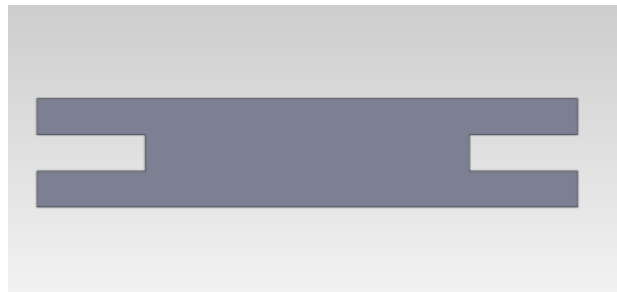


Figure 28: Component B Side Profile

Figure 28 above shows the side profile of one of two tracks fixed to the lid of the culture dish, attached using a catalytic epoxy. The tracks are 30mm long and 6 mm high and feature two 2 mm grooves on either side that allow a space for component C. As shown in Figure 29 below, a hole is drilled through the center of the entire part so that component C can move within the tracks.

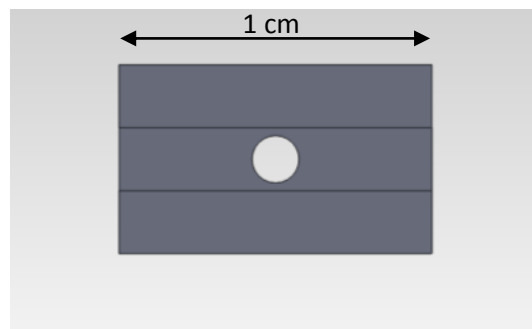


Figure 29: Component B Front Profile

### *Component C- Slider*



Figure 30: Component C Top-Down View

Component C shown in Figure 30 above consists of two rectangular bars connected by two cylindrical rods. The rectangular bars fit into the grooves of Component B, and the rods fit through the holes that extend through Component B. The bottom bar (closest to edge of culture dish) has a notch that allow for attachment of a magnet. The upper bar has 4 holes spaced 15 mm apart for the attachment of metal pins that extend downward (into paper). These pins provide the second attachment point for the tissue constructs below. Based on the attraction between the magnet attached to the bottom bar and the magnet attached to the motor outside of culture, Component C moves within Component B to provide 1 mm of stretch (10% strain) to the tissue construct. Small rubber bands will be attached between the stationary posts and component C to ensure that the sliders return to their initial position after being stretched by the magnet. Figure 31 below shows both components B and C together. Both parts are laser cut from acrylic using the WPI machine shop facilities, with the exception of the rods connecting the two ends of Component C, which are found commercially.

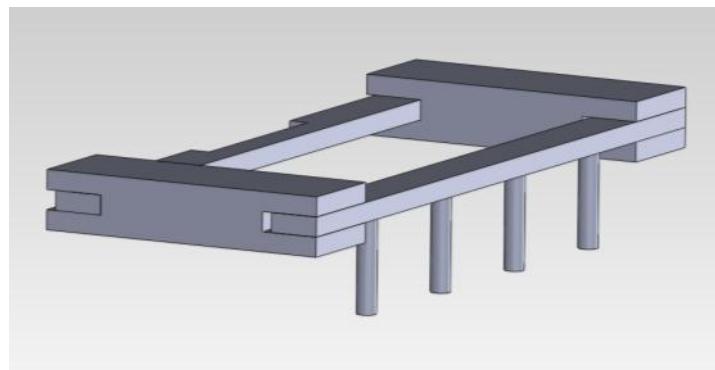
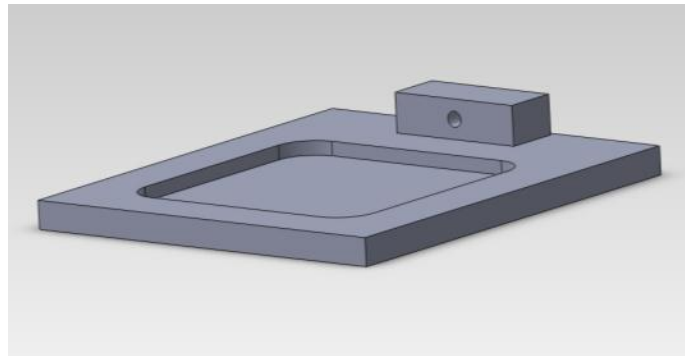


Figure 31: Components B and C



### *Component D- Stabilizing Base*



**Figure 32: Component D Stabilizing Base**

Component D, as shown in Figure 32 above, is a stabilizing base for the culture dish. The system must be stabilized so that when actuation takes place the culture dish does not move to contact the outer magnet completely. Component D also features a block for the mounting of the motor-magnet system. The block has a hole drilled through the center, which is precisely aligned with the height of the magnet inside the culture dish. This design feature allows for the correct magnet alignment no matter the dimensions of the selected motor, as the motor can be mounted to the back of the base, and the moving shaft can extend through the hole.

### *Component E- Stepper Motor*

In order to run the device and provide mechanical stimulation to the tissue, a motor was needed. The team first considered a linear actuating motor that would simply move back and forth and had the controller located inside the motor. A picture of this motor can be seen below in Figure 33. The fact that the controller was already part of the motor was the reason the team initially pursued that idea. However, challenges were observed in attempting to mount the motor to the base. The long, narrow shape of the motor proved too difficult to mount in place while still providing a straight connection between the two magnets. Another problem with this motor was the actuating end, which had a rigid surface that was difficult to mount a magnet to. For these reasons, the team decided to look into a different motor.





Figure 33: Linear Actuating Motor

The next type of motor that was considered was a stepper motor. This motor would allow for the control of how fast the actuating arm moved horizontally, as well as how far it extended. The end of the actuating part was threaded, which allowed for the attachment of a small piece of wood to which the magnet could then be glued. The motor is shown below in Figure 34. This was ideal because it also allowed for some flexibility in making sure that the connection between the two magnets was properly aligned.



Figure 34: Portescap Stepper Can Stack Motor

## 5: Design Verification

From the preliminary design, the team moved forward to testing and verifying aspects of the design. The following sections describe these tests and any resulting iterations that ultimately led to the final design.

### 5.1: Mold Designs

Due to the limitations discovered during feasibility studies for the dog-bone mold design, the team decided to move forward towards a simpler molding concept. The small height of the commercial culture dish (15 mm) also pointed toward a two-step system in which tissue could be formed in a separate environment and then mounted onto the anchor points in the mechanical stimulation device. A mold featuring 20 mm long V-shaped channels in an oval configuration was created and milled from polycarbonate using a CNC machine located in Higgins Laboratories. The SolidWorks representation of the mold and the actual mold are shown side by side in Figure 35 below.

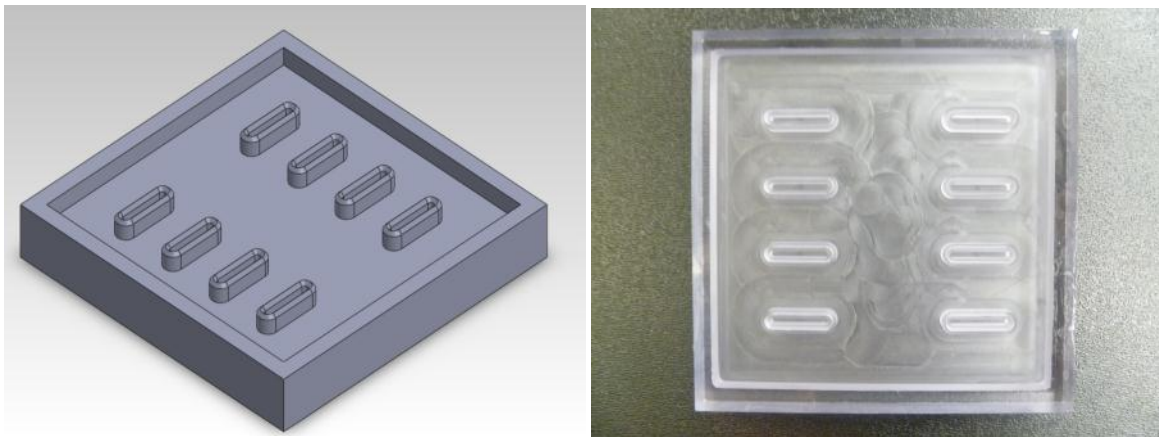


Figure 35: SolidWorks representation and image of actual oval-shaped mold

Once the polycarbonate mold was created, a 2.5% agarose/DMEM solution was poured into the depression to create the channels for cell seeding. While tissue formed within the channels shortly after seeding, the constructs soon broke. The team posited that this could be due to stress created at the curved ends of the channels or imperfections in the V-shaped depressions as a result of the polycarbonate milling process. The team anticipated that the mold could be compatible with the use of an extracellular matrix component to provide additional structural integrity for the tissue construct, but was not conducive to the delicate tissues created solely by cell-mediated assembly.

Because of the project's focus on self-assembled tissue, the team moved forward with a circular mold developed by Gwyther, et al. (2011), in which it was expected that any forces could be distributed

evenly around a central agarose post. These molds had already been demonstrated to aid in the formation of smooth muscle tissue constructs, making them a good candidate to allow for the development of self-assembled tissue rings from both C2C12 and human primary skeletal muscle cells.

## 5.2: Culture Dish Fabrication and Assembly

The design described in Chapter 4 required several iterations in terms of assembly techniques and design modifications. This section describes these techniques and the preliminary tests that were used to make informed changes to the preliminary design.

The first modification to the preliminary design was a result of the manufacturing limitations of the laser-cutter system. Since the laser-cutter can only create parts from a 2D drawing, with the third dimension controlled by the thickness of the material, the original two track system was redesigned to include four laser cut acrylic tracks with two placed closely together in parallel on either end of the lid of the dish. This also resulted in a modification to the slider design, which was altered to consist of one continuous piece, where acrylic connectors built into the 2D drawing replace the rod connectors of the preliminary design. This modification reduces the complexity of the design in terms of both assembly and materials used.

Once the tracks and slider were fabricated using the laser-cutter and 0.080" acrylic, a ceramic magnet was attached to the slider and all parts were clamped together in their functional form and fixed to the top of the culture dish using a fast-drying epoxy. Once the epoxy had cured, the clamps were removed. A small spring was fixed to the front of the slider and the lid of the dish using a combination of epoxy and small stainless steel strips for additional strength. An initial test was performed by holding a strong magnet outside of the edge of the dish closest to the internal magnet. While the magnetic attraction was apparent, there was obvious contact friction between the tracks and slider that impeded free movement of the system. Upon examining the parts more closely, it was noted that the slider piece had bowed during fabrication due to the thin parts and the heat of the laser used in their fabrication. The slider was redesigned to feature two more connecting pieces for additional structural support. The new slider was manufactured using the laser-cutter and there was no apparent bowing in the new design. A SolidWorks drawing of the new slider is shown in Figure 36 below.

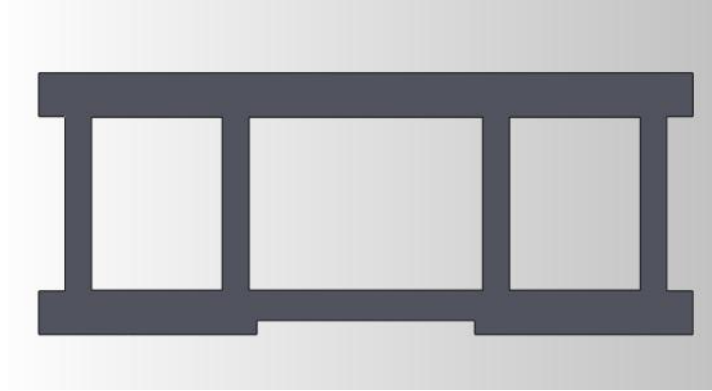


Figure 36: 2D View of Redesigned Slider

A second assembly was created using the same technique described previously, and the slider was found to move freely along the tracks. The spring successfully returned the slider to its original position once the external magnet was out of range.

With the track-slider system functioning as intended, a check was performed to compare the displacement of the slider in the actual assembly to the prescribed displacement of 2 mm. The slider was moved into its expanded position using the external magnet and the displacement was measured using calipers. The actual displacement was found to be approximately 2.5 mm. This discrepancy was due in part to the heat of the laser creating imperfections in such small parts during fabrication, as well as limitations in assembly precision by the assembler. More assemblies were created, and displacement was found to vary to within a range of approximately  $\pm 0.5$  mm from the intended 2 mm expansion. While this represents a considerable amount of error, the team decided to move forward with the design because of its low cost and manufacturability. While a precise control of strain would be ideal within a single device, the team decided that it would still be valuable to study the effects of a less precise cyclic stretch on tissue constructs, and that simple modifications to the dimensions of the parts could allow for a certain level of control of the strain imparted to the tissue construct during mechanical stimulation.

Attention was then turned to the mounting of the anchoring points on the front of the slider and the lid of the dish. Stiff stainless steel wire was selected as the material for the anchoring points. The wire was cut into small pieces and each was bent into an L shape. The part of the wire corresponding to the bottom of the L was then attached to the slider and the lid of the dish using a fast-drying epoxy. Once the epoxy set completely, the pins were found to have a sufficiently strong attachment to the acrylic slider and polystyrene dish.

### 5.3: Base Design and Fabrication

Initially, the base was designed to be milled from a solid piece of polycarbonate. However, due to limitations in both time and budget, the team decided to manufacture the base by layering the same 0.080" acrylic used for the track-slider system. The appropriate layers were manufactured using the laser-cutter, and then stacked together using a spray adhesive. Due to the imprecision of the laser-cutter, and the slight inclines on the sides of the culture dish, the well for the dish was slightly small. To address this, the sides were expanded by hand using a razor blade until the bottom of the dish fit securely in the well. Figure 37 below shows the completed base.

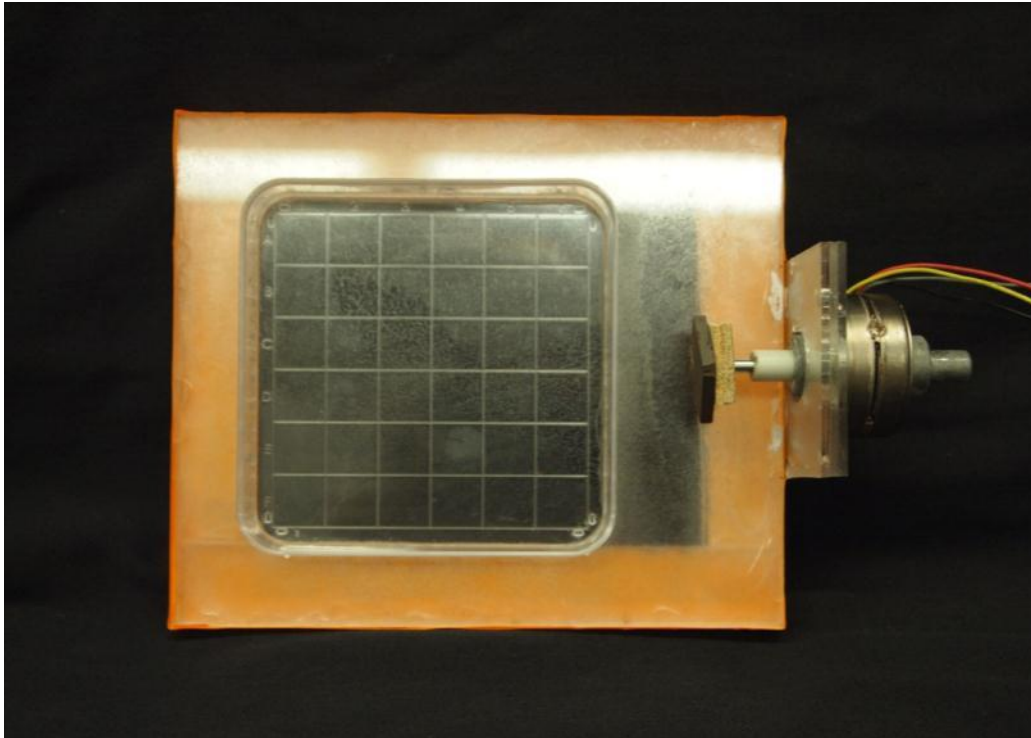


Figure 37: Assembled base

While this design proved to be acceptable for short term testing, the humidity of the incubator seemed to deteriorate the bonds between the acrylic parts. Because of time constraints, the team reinforced the base with tape, as seen in orange on the Figure above.

### 5.4: Evaluation of Tissue Constructs

Tissue constructs seeded in the 2 mm post diameter rings with 500,000 C2C12 cells were evaluated for their myogenic properties. H&E staining shown in Figure 25 determines that rings seeded

with a higher number of cells were more robust and easy to handle. These tissue constructs also showed myotube formation as evidenced by multinucleated fibers.

In order to further evaluate the myotube formation in the 3D tissue, the rings formed by C2C12 cells were fixed and sectioned for immunohistochemistry. A myosin stain was conducted on sections to label myosin protein expression in mature muscle fibers. Figure 38 (right) shows that some myosin was expressed in 3D rings 9 days post differentiation. However, a majority of the cells in the ring did not express myosin. The C2C12 cells showed more myosin expression in 2D culture. Figure 38 (left) illustrates C2C12 cells grown in 2D culture with 6 days allowed for differentiation. The fibers formed in 2D culture are longer and denser than the fibers formed in 3D culture.

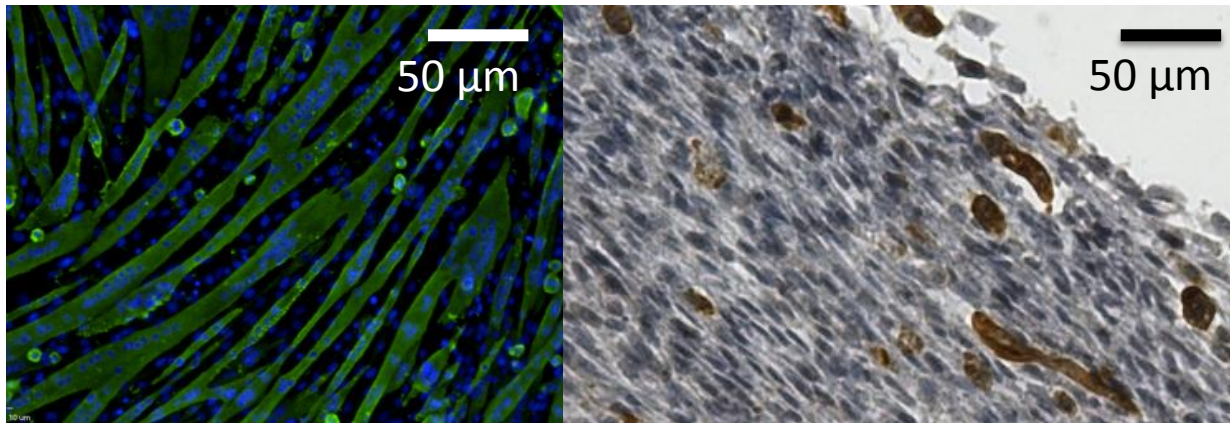


**Figure 38: Difference in Myosin Expression from 2D to 3D Culture**  
(left) C2C12 cells in 2D 6 days post differentiation: Myosin counterstained with Hoescht  
(right) C2C12 cells in 3D 9 days post differentiation: Myosin counterstained with Hemotoxylin

## 6: Final Design

### 6.1: Final Device

The following sections outline the final design and procedure for using the device. A detailed description of each component of the device is given, along with pictures of the components. The last section describes the assembly of the motor and the parts responsible for its control.

#### 6.1.1: Final Device Design

After making adjustments to the design of the mechanical stimulation device, the final design can be seen below in Figure 39.

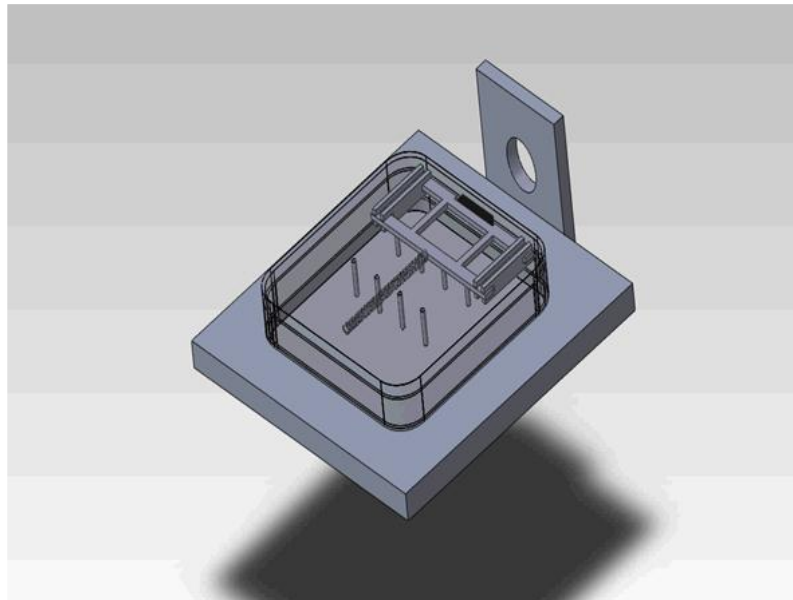
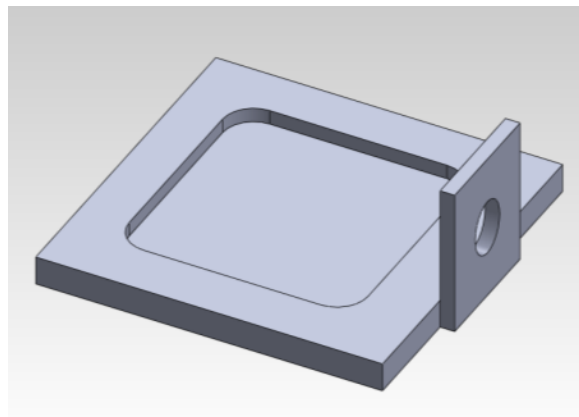


Figure 39: Final Design for Mechanical Stimulation Device

This design incorporates a magnetic, track-slider system whose motion is controlled by a stepper motor. All the pieces of the device seen inside the culture dish are fixed to the lid in order to keep them isolated from the tissue and medium. This prevents contamination and allows for simple sterilization using UV light. The concept of using the attraction between two magnets to move the slider and provide mechanical stimulation to the tissue construct is quite simple, and adds an additional level of isolation between the sensitive environment of the media and tissue in the dish and the actuating mechanism. The actuating arm of the stepper motor has a magnet attached as described above. When the arm

extends outward toward the culture dish, this magnet eventually attracts the magnet that is placed inside the dish. Once the two magnets are attracted, the slider will be pulled in the direction of the motor; the tracks allow for control of this movement. When the slider is shifted, the pins attached to it will move as well, creating distance between the moving and stationary pins. This will ultimately stretch the tissue that is anchored around the two sets of stainless steel pins.

The base of the device is made from layered acrylic. The top layer has a notch cut out that has the same dimensions as the bottom of the culture dish. This indentation provides a place for the culture dish, ensuring that it remains stationary while mechanical stimulation is taking place. The component on the right with the circular hole allows for mounting of the stepper motor. The pieces that were used to make the base are held together using glue specifically for acrylic, provided by the machine shop in the Higgins Laboratory. A picture of the SolidWorks model can be seen below in Figure 40.



**Figure 40: SolidWorks Representation of Layered Acrylic Base**

The first anchoring point for the tissue construct is provided by four stainless steel pins that are attached to the lid of the dish using an epoxy, as seen in Figure 41. These pins remain stationary during stimulation and extend down into the media that is present in the bottom of the dish.



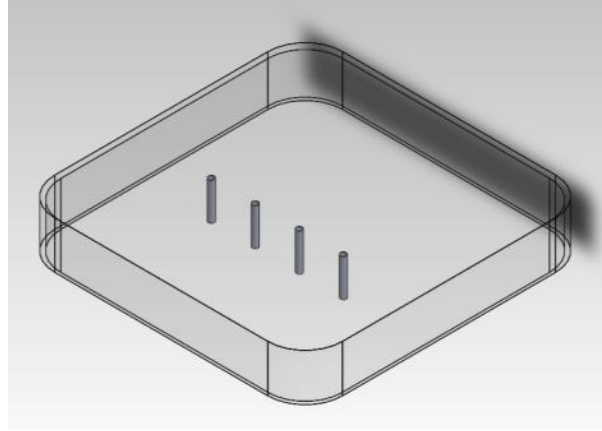


**Figure 41: Lid of the Culture Dish with Attached Pins**

The track for this system is comprised of four laser-cut acrylic pieces. They are each 30 mm long and 2 mm thick. Also fixed to the lid of the dish, these pieces each have a 2 mm notch cut out on either side that allows for the movement of the slider piece back and forth.

The slider piece is also made from acrylic and was fabricated using the laser cutter (Figure 42). On one side of the slider, four stainless steel pins are fixed using epoxy. These pins are the second anchoring point for the tissue construct and also extend downward into the media that resides at the bottom of the culture dish. These pins are displaced with the slider when mechanical stimulation is taking place. On the other side of the slider, there is a notch cut out for the placement of a magnet. This magnet is fixed inside the notch with epoxy and does not come in contact with the side of the culture dish.

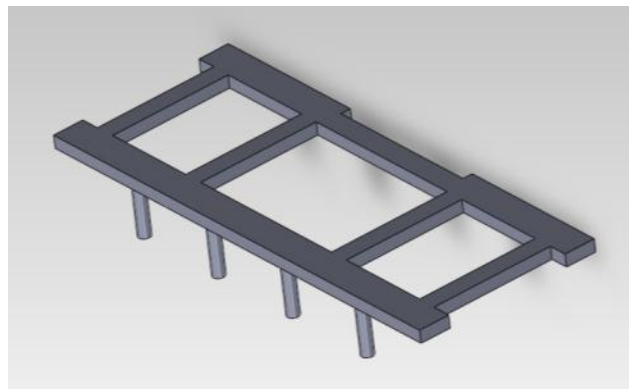


**Figure 42: Slider with Mounting Pins and Notch for Magnet**

The purpose of the spring in this device assembly is to simply recall the slider back to its original position once the two magnets are no longer attracted to each other. We found that the tissue alone

was not capable of pulling the slider back and therefore added a spring to put tension on the slider to bring it back to its initial position.

### 6.1.2: Final Device Assembly

Once the parts of the device that reside inside the dish are assembled, the overall assembly is almost complete. The stepper motor must be mounted to the base of the dish either with screws or glue. The team found that glue was sufficient for securing the motor to the acrylic base. The final aspect of device assembly involves the configuration of the stepper motor's controller and driver.

An Arduino Megaboard Controller and a Sparkplug Easy Driver were purchased, both of which can be seen below in Figure 43. These components were suggested to us by our co-advisor as an inexpensive and simple way to control the stepper motor. Using schematics, the four wires of the stepper motor were connected in series to the sparkplug driver. The ground and two power wires of the driver were then inserted into their respective pins on the controller. Again using online schematics to find the correct placement, the STEP wire of the driver was placed in pin #3 of the controller, the ground wire to the ground pin, and the DIR wire to pin #22 of the controller. Next, the controller was plugged into a laptop using a printer cable. We were fortunate to have been given a portable power supply from the Robotics Engineering Department for the duration of our project. This allowed us to run the device in the appropriate setting and eliminated the cost of purchase for this component. The red lead of the power supply was connected up to the M+ wire of the driver and the ground lead of the power supply to the ground wire of the driver. The circuit was then complete.

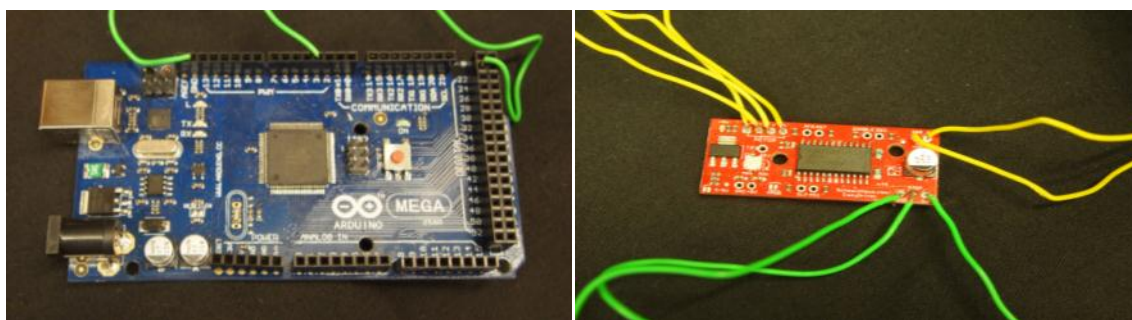


Figure 43: (Left) Arduino Controller and (Right) Sparkplug Easy Driver

In order to run the motor, the Arduino Software was downloaded from the Arduino website. A code was then created to run the motor. The code can be seen below in Figure 44. When this code is entered into the software and uploaded, the controller is programmed and communicates with the motor. The power supply voltage was set to 8V. Once the power is turned on, the motor runs according to the code.

```

#define DIR_PIN 2
#define STEP_PIN 3

void setup() {
  pinMode(DIR_PIN, OUTPUT);
  pinMode(STEP_PIN, OUTPUT);}
void loop(){
  //rotate a specific number of microsteps (16 microsteps per step)
  rotate(5400, .5);
  delay(10);

  rotate(-5400, .25); //reverse
  delay(10);}

void rotate(int steps, float speed){
  //rotate a specific number of microsteps (16 microsteps per step) - (negative for reverse movement)
  //speed is any number from .01 -> 1 with 1 being fastest - Slower is stronger
  int dir = (steps > 0)? HIGH:LOW;
  steps = abs(steps);

  digitalWrite(DIR_PIN,dir);

  float usDelay = (1/speed) * 70;

  for(int i=0; i < steps; i++){
    digitalWrite(STEP_PIN, HIGH);
    delayMicroseconds(usDelay);

    digitalWrite(STEP_PIN, LOW);
    delayMicroseconds(usDelay);}}

```

Figure 43: The Arduino code used for running the stepper motor

The number of steps that the motor took to fully extend outward could be adjusted in the code. This ultimately changed the pace at which the actuating arm extended and retracted. Due to the nature of the magnetic attraction system in place, the team adjusted the code in order to find a frequency that provided reasonable cyclic stretch of the tissue construct. Due to a lack of consensus within the literature concerning timing protocols, the team decided on a frequency of 0.25 Hz for initial testing.

## 6.2: Final Method for Tissue Construct Formation

The subsections below outline the final method established for seeding either C2C12 or primary human skeletal muscle cells into ring-shaped molds to form the tissue constructs for use with the device. These methods consistently resulted in production of continuous and uniform tissue constructs.

### 6.2.1: C2C12 Cell Line

Cells from the C2C12 line, an established and immortalized mouse myoblast cell line, were maintained and differentiated as described in section 4.2: Cell Culture Methods. 48 hours after differentiation was initiated, cells were detached from the tissue culture vessel through a brief wash with PBS and incubation with 0.025% trypsin in PBS for 10 minutes. The cells were then centrifuged at 1000rpm for 5 minutes and resuspended to a concentration of  $5 \times 10^6$  cells/mL in differentiation medium (components as previously described). The cell suspension was then seeded into the wells of the agarose ring mold. Small diameter wells (2mm) were seeded with 100uL of cell suspension, or 500,000 cells/well; medium diameter wells (4mm) were seeded with 200uL of cell suspension, or  $1 \times 10^6$  cells/well; and large diameter wells (6mm) were seeded with 300uL of cell suspension, or  $1.5 \times 10^6$  cells/well. Fresh differentiation medium was added to all wells at 24 hours post-seeding, and changed as needed to maintain tissue integrity.

### 6.2.2: Human Skeletal Muscle Primary Cells

Primary human skeletal muscle cells were also used to form tissue constructs. The primary cells used were not fully characterized at the time of this project, but were known to contain two distinct subpopulations: a population of attached cells that exhibited highly myogenic properties, and a population of suspension cells that behaved much like satellite cells. These suspended cells were self-renewing, but when subcultured, a fraction of the population would also attach to the tissue culture vessel to establish the highly myogenic population. Because the attached population of cells was so highly myogenic, differentiation was not initiated prior to seeding the cells into the agarose molds.

To seed the cells into the agarose molds for tissue construct formation, the suspended population of cells was first removed and set aside to maintain the cell line. The remaining attached population of cells was then washed with PBS and incubated with 0.025% trypsin in PBS until the cells detached, approximately 2 minutes. The trypsin was then neutralized with the same medium used to maintain the cells, and the suspension was centrifuged at 1000rpm for 10 minutes. The cells were then resuspended to a concentration of  $5 \times 10^6$  cells/mL in the maintenance medium. The cell suspension was then seeded into the wells of the agarose ring mold at the same concentrations used to form C2C12 tissue constructs: small diameter wells (2mm) were seeded with 100uL of cell suspension, or 500,000 cells/well; medium diameter wells (4mm) were seeded with 200uL of cell suspension, or  $1 \times 10^6$  cells/well; and large diameter wells (6mm) were seeded with 300uL of cell suspension, or  $1.5 \times 10^6$  cells/well.

cells/well. Fresh medium was added to all wells at 24 hours post-seeding, and changed as needed to maintain tissue integrity.

## 7: Discussion

### 7.1: Device Discussion

Although the team was not able to retrieve data from the mechanical stimulation part of our project, we were able to successfully mount the tissue to the anchoring pins and stretch the tissue inside the incubator, with no contamination, and maintained tissue viability. The self-assembled tissue proved difficult to handle and often broke in the process of mounting it to the pins. While all of the device's parts are relatively inexpensive, an overall lack of precision in manufacturing and necessary assembly techniques was responsible for limited user-control on the levels of strain that the tissue will see during stimulation. Additionally, over time in the tissue culture environment, high levels of humidity begin to affect the bonds of the epoxies, resulting in compromised integrity of the track-slider system. This issue does not affect stretch protocols with a duration of one week or less, as a new sterile culture dish should be created for each new experiment. In order to run longer term experiments, however, this design flaw would need to be corrected.

### 7.2: Tissue Discussion

Self-assembled tissue formation using either immortalized C2C12 cells or primary human skeletal muscle cells was successful in the Rolle agarose ring mold design. C2C12 cells produced tissue rings that remained viable and structurally intact for up to 1 week post-seeding (the longest period they were studied for). The primary human skeletal muscle cells formed tissue that was viable for up to 5 days post-seeding but then broke apart. Tissue formation using C2C12 cells in the oval agarose mold with the v-shaped channel was successful; however, the tissue did not remain intact for more than 12 hours. Similar results were observed by Kalluri et al. (2011) in the dog-bone shaped mold. The Rolle ring design was likely to have sustained the tissue for longer periods of time because it evenly distributed the passive tension that occurred once the tissue self-assembled and was able to contract. Both the dog-bone and oval mold designs contained points at which stress during tissue contraction was concentrated. In the dog bone mold, the stress is concentrated at the point in which the circular portion meets the straight portion on both ends of the mold. The oval mold contains stress points at both ends of the oval. These points were areas of concentrated stress under which the tissue was most likely to break, as it was not strong enough during initial development to withstand this stress.

The Rolle rings were not 100% effective in maintaining tissue integrity for 1 week. Some tissue rings formed successfully but then broke within 12- 48 hours after seeding at two days post serum-

induced differentiation (see Figure 24). These tissue rings may have broken due to a lack of matrix support and myotube formation.

When the self-assembled tissue from the Rolle ring mold was evaluated through histological sectioning, several trends were observed. H&E staining, shown in Figure 25, showed that lower seeding densities exhibited better nuclear and cell alignment than the higher seeding densities. This may be due to improved nutrient diffusion in smaller diameter tissue, which would allow all cells in the tissue to receive the proper signals for differentiation. Additionally, myosin expression staining shown in Figure 33 indicates decreased myosin expression from 2D to 3D culture at the same time point. This decrease may be due to a lack of signaling mechanisms that exist in the *in vivo* environment and assist in differentiation, or a need for longer culture periods to attain the same level of differentiation in a more complex 3D structure.

## 8: Conclusions and Recommendations

### 8.1: Device Conclusions

Overall, the device allowed for the successful anchoring and cyclic stretch of self-assembled skeletal muscle tissue constructs within the constraints of the tissue culture environment. The device was easily sterilizable via ethanol and UV methods, and the isolation of moving parts and epoxies allowed for flexibility of material choice while preventing any contamination and allowing for prolonged tissue viability. The extensive use of acrylic, along with laser-cutting as a primary manufacturing technique, drove down the device cost and allowed for a large amount of flexibility in terms of rapid design modifications and testing. While the device was safe, its user friendliness and time efficiency represent its greatest weaknesses, as a number of small fragile parts must be assembled by hand with great care and attention to detail.

### 8.2: Tissue Conclusions

The device design achieved the initial objective of allowing evaluation of tissue properties. Following tissue formation in the mold design, the tissue was evaluated through histological sectioning. These sections could then be assessed for internal structure and alignment through a hemotoxylin and eosin (H&E) stain. Expression of myosin protein could be observed through a myosin stain, which is indicative of myotube formation and is a marker for differentiation in skeletal muscle. These properties could also be evaluated following different courses of mechanical stimulation. Additionally, after removing the tissue construct from the mold or mechanical stimulation device, the tissue could be evaluated for mechanical properties such as contractibility and structural integrity. Contractibility could be measured by applying a current to the tissue construct and measuring the strength of the response twitch. The structural integrity could be measured using an Instron machine for pull-to-failure testing. This will provide a stress vs. strain curve that can be interpreted for tissue stiffness and ultimate tensile strength.

Tissue construct formation using both C2C12 and primary human skeletal muscle cell lines was successful using the Rolle ring agarose mold design. The ring design facilitated self-assembly of tissue constructs without the assistance of extracellular matrix scaffolds. Ring formation was observed using cell seeding concentrations ranging from 2.33 to 6 million cells per ml. Additionally, both human myoblasts and C2C12 cells were able to form tissue rings with diameters of 2 mm, 4 mm, and 6 mm. This tissue remained structurally intact and viable in static culture for up to 1 week.



Tissue ring formation using oval mold design facilitated self-assembly of tissue as well; however, it did not support long-term culture. Initial formation of tissue constructs in oval molds was successful, but upon initial contraction the tissue constructs broke under their own tension. This suggests that the tissue lacked structural integrity in early development. This may be due to lack of matrix formation or myotube formation.

### 8.3: Device Recommendations

There are several recommendations for the design and usage of the mechanical stimulation device created over the course of this project. First of all, we recommend that the placement of the stationary pins should be moved from the lid of the dish to the bottom. While this calls for the additional use of a non-cytotoxic glue, the current position of the pins allow for the tissue to simply fall off and into the bottom of the dish, especially when media changes are necessary.

Another problem that we faced was the matter of transferring the tissue from the mold to the device. This allowed for more human error and breakage of the fragile tissue. We therefore recommend reducing the amount of handling of the tissue. This could be done by creating a molding system that fits in the culture dish, thus minimizing to handling of the rings. The pins could be placed into the agarose mold and when the tissue self assembles, it could be gently moved directly upwards onto the pins.

As the device is now, it is difficult to provide fine control and adjustment of the percent strain to the tissue construct. This could be addressed by both redesigning and finding a more precise way of machining and assembling the parts. If a high level of precision could be achieved, parts such as stoppers or spacers within the track slider system could be viable. Thus, outsourcing to facilities with more precise machine tools than those found in the WPI shops should be considered. More precision could also be achieved by further calibrating the system through continued experimentation, especially in the area of magnet choice and stepper motor control. We would also like to recommend that in future iterations, the device should be modified for its amenability to electrical stimulation. If this amenability is achieved, contractile function of the tissue could possibly evaluated within the device, based on monitoring the deflection of the anchoring points when electrical stimulation is taking place.

Lastly, the timing between tissue formation and mechanical stimulation should be investigated. Experiments to determine at what time after the formation of the self-assembled tissue rings mechanical stimulation should be provided would be ideal. This could provide better tissue properties and rings with more structural integrity.

## 8.4: Tissue Recommendations

For future experimentation, we recommend looking into methods for improving the mechanical strength of the tissue construct, specifically during early development. The main issue identified with the tissue constructs was fragility of the tissue when handled. In many cases, the tissue also broke from its own passive tension before it could be moved to the mechanical stimulation device.

In order to improve the structural properties of the tissue and encourage increased myotube formation, we recommend evaluating several parameters that may have a positive effect on these properties. These recommendations are based upon the knowledge that satellite cells do not exist in pure population *in vivo*. Rather, they depend on cell-cell interactions, growth factor signaling, and extracellular matrix deposition (Ten Broek et al., 2010).

First, we recommend the use of serum free cultures and growth factor supplements such as IGF, FGF, and HGF, which may improve myotube formation (Gawillita et al., 2008. Ten Broek et al., 2010.). Additionally, the use of extracellular matrix proteins as a scaffold or basement coating within the agarose molds may provide both support and important integrins for differentiation (Ten Broek et al., 2010. Lawson et al., 2000. Page et al., 2011).

Lastly, we recommend experimentation with co-culture of myoblastic cells with other cell types found in skeletal muscle *in vivo*. Co-culture with neurons, blood vessels, or fibroblast cells may all prove to be beneficial. These three components are naturally present in skeletal muscle and interact with skeletal muscle cells to provide important signaling mechanisms for muscle formation (Ten Broek et al., 2010. Larkin et al., 2006. Levenberg et al., 2005). We suggest a primary focus on fibroblasts because they deposit extracellular matrix, which will in turn provide support for the tissue as it self-assembles and thus address the issues with inadequate mechanical strength and structural integrity as the tissue develops.

## 8.5: Impact

The final design is a feasible, functional device for the mechanical stimulation of developing engineered skeletal muscle tissue that has potential for future improvement and optimization. With further development, this design has the potential to have a significant impact on the field of skeletal muscle tissue engineering. By providing a means to mechanically stimulate skeletal muscle tissue during development using different courses of cyclic stretch, the device produces tissue that is one step closer to skeletal muscle *in vivo*. An accurate model of skeletal muscle formation and function is crucial to understanding its developmental process, both normally and in myopathic tissue. Such a model could

not only be used to further the understanding of the mechanisms of skeletal muscle development, but also to identify drug targets, investigate the effect of possible treatments, and provide other valuable preclinical data. As a mechanical stimulation device, it also has cross-applications in developing vascular tissue and directing differentiation in human mesenchymal stem cells, as well as any other tissue that requires mechanical cues during development, regeneration, or maturation.

## References

- Muscular Dystrophy Association (2011). Muscular Dystrophies Retrieved September 25, 2011, from <http://www.mda.org/disease/>
- Awiss, K. J., Gough, J. E., & Downes, S. (2010). Aligned electrospun polymer fibres for skeletal muscle regeneration. *European cells & materials*, 19(Journal Article), 193-204.
- Beier, J. P., Stern-Straeter, J., Foerster, V. T., Kneser, U., Stark, G. B., & Bach, A. D. (2006). Tissue engineering of injectable muscle: three-dimensional myoblast-fibrin injection in the syngeneic rat animal model. *Plastic and reconstructive surgery*, 118(5), 1113, 0032-1052.
- Bian, W., & Bursac, N. (2008). Tissue engineering of functional skeletal muscle: challenges and recent advances. *IEEE engineering in medicine and biology magazine: the quarterly magazine of the Engineering in Medicine & Biology Society*, 27(5), 109.
- Brunelli, S., & Rovere-Querini, P. (2008). The immune system and the repair of skeletal muscle. *Pharmacological Research*, 58, 117-121.
- Buckingham, M., Bajard, L., Chang, T., Daubas, P., Hadchouel, J., Meilhac, S., . . . Relaix, F. (2003). The formation of skeletal muscle: from somite to limb. *Journal of Anatomy*, 202(1), 59-68.
- Camargo, F. D., Green, R., Capetenaki, Y., Jackson, K. A., & Goodell, M. A. (2003). Single hematopoietic stem cells generate skeletal muscle through myeloid intermediates. *Nature medicine*, 9(12), 1520-1527.
- Charge, S., & Rudnicki, M. (2004). Cellular and Molecular Regulation of Muscle Regeneration. *Physiological Reviews*, 84(1), 209-238.
- Ciciliot, S., & Schiaffino, S. (2010). Regeneration of Mammalian Skeletal Muscle: Basic Mechanisms and Clinical Implications. *Current Pharmaceutical Design*, 16, 906-914.
- Das, M., Gregory, C. A., Molnar, P., Riedel, L. M., Wilson, K., & Hickman, J. J. (2006). A defined system to allow skeletal muscle differentiation and subsequent integration with silicon microstructures. *Biomaterials*, 27(24), 4374-4380.
- Drury, J. L., & Mooney, D. J. (2003). Hydrogels for tissue engineering: scaffold design variables and applications. *Biomaterials*, 24(24), 4337-4351.

- Gawlitta, D., Boonen, K. J. M., Oomens, C. W. J., Baaijens, F. P. T., & Bouten, C. V. C. (2008). The influence of serum-free culture conditions on skeletal muscle differentiation in a tissue-engineered model. *Tissue Engineering Part A*, 14(1), 161-171, 1937-3341.
- Grefte, S. e. a. (2007). Skeletal Muscle Development and Regeneration. *Stem Cells and Development*, 16, 857-868.
- T. A. Gwyther, J. Z. Hu, K. L. Billiar and M. W. Rolle. (2011) Directed cellular self-assembly to fabricate cell-derived tissue rings for biomechanical analysis and tissue engineering.
- Huang, Y.-C., Larkin, L., Dennis, R. G., & Baar, K. (2005). Rapid formation of functional muscle in vitro using fibrin gels. *Journal of Applied Physiology*, 98(2), 706-713.
- Kalluri, D. S. a. B. E., Donado, C. A. S. a. B. E., Bhagat, S. S. S. a. I. D., Page, R. L. F. a. B. B., & Adams, D. S. F. a. B. B. (2011). *Design of a molding system to recapitulate skeletal muscle fiber*. Worcester, MA: Worcester Polytechnic Institute.
- Khodabukus, A., Paxton, J. Z., Donnelly, K., & Baar, K. (2007). Engineered muscle: a tool for studying muscle physiology and function. *Exercise and sport sciences reviews*, 35(4), 186, 0091-6331.
- Kleinman, H. K., & Martin, G. R. (2005). Matrigel: Basement membrane matrix with biological activity. *Seminars in cancer biology*, 15(5), 378-386.
- Koning, M., Harmsen, M. C., van Luyn, M. J. A., & Werker, P. M. N. (2009). Current opportunities and challenges in skeletal muscle tissue engineering. *Journal of tissue engineering and regenerative medicine*, 3(6), 407-415.
- Kroll, T. G., Peters, B. P., Hustad, C. M., Jones, P. A., Killen, P. D., & Ruddon, R. W. (1994). Expression of laminin chains during myogenic differentiation. *Journal of Biological Chemistry*, 269(12), 9270, 0021-9258.
- Larkin, L. M., Van Der Meulen, J. H., Dennis, R. G., & Kennedy, J. B. (2006). Functional evaluation of nerve-skeletal muscle constructs engineered in vitro. *In Vitro Cellular & Developmental Biology-Animal*, 42(3), 75-82, 1071-2690.

- Lawson, M. A., & Purslow, P. P. (2000). Differentiation of myoblasts in serum-free media: effects of modified media are cell line-specific. *Cells Tissues Organs*, 167(2-3), 130-137, 1422-6405.
- Levenberg, S., Rouwkema, J., Macdonald, M., Garfein, E. S., Kohane, D. S., Darland, D. C., . . . D'Amore, P. A. (2005). Engineering vascularized skeletal muscle tissue. *Nature biotechnology*, 23(7), 879-884, 1087-0156.
- Liao, H., & Zhou, G.-Q. (2009). Development and progress of engineering of skeletal muscle tissue. *Tissue engineering. Part B, Reviews*, 15(3), 319-331.
- Lieber, R. L. (1999). *Skeletal Muscle is a Biological Example of a Linear Electro-Active Actuator*. Paper presented at the 6th Annual International Symposium on Smart Structures and Materials, San Diego, California.
- Liu, Y., Ramanath, H. S., & Wang, D.-A. (2008). Tendon tissue engineering using scaffold enhancing strategies. *Trends in biotechnology*, 26(4), 201-209.
- Mann, V., Adams, A., Kogianni, G., Simpson, A., Goldspink, G., & Noble, B. S. (2006). Mechano growth factor expression in bone: Response to mechanical stimulation. *JOURNAL OF BONE AND MINERAL RESEARCH*, 21(7), 1171-1171.
- Moon, D. G., Christ, G., Stitzel, J. D., Atala, A., & Yoo, J. J. (2008). Cyclic mechanical preconditioning improves engineered muscle contraction. *Tissue engineering. Part A*, 14(4), 473-482.
- Neas, J. F. (2003). *Muscular System: Myogenesis*: Pearson Education, Inc.
- Powell, C. A., Smiley, B. L., Mills, J., & Vandeburgh, H. H. (2002). Mechanical stimulation improves tissue-engineered human skeletal muscle. *American Journal of Physiology-Cell Physiology*, 283(5), C1557, 0363-6143.
- Saltzman, W. M. (2009). *Biomedical Engineering: Bridging Medicine and Technology*. New York: Cambridge University Press.
- Schiaffino, S., & Partridge, T. (2009). *Skeletal Muscle Repair and Regeneration*: Springer.
- Shi, X., & Garry, D. (2006). Muscle stem cells in development, regeneration, and disease. *Genes and Development*, 20, 1692-1708.

Standley, L. J. (2000). The Muscular System, from  
[http://www.drstandley.com/bodysystems\\_muscular.shtml](http://www.drstandley.com/bodysystems_muscular.shtml)

Stern-Straeter, J., Bran, G., Riedel, F., Sauter, A., Hörmann, K., & Goessler, U. R. (2008). Characterization of human myoblast cultures for tissue engineering. *International journal of molecular medicine*, 21(1), 49-56, 1107-3756.

Ten Broek, R. W., Grefte, S., & Von den Hoff, J. W. (2010). Regulatory factors and cell populations involved in skeletal muscle regeneration. *Journal of cellular physiology*, 224(1), 7-16, 1097-4652.

Turner, N., & Badylak, S. (2011). Regeneration of Skeletal Muscle. *Cell and Tissue Research*, ePub ahead of print.

Vachon, P. H., Loechel, F., Xu, H., Wewer, U. M., & Engvall, E. (1996). Merosin and laminin in myogenesis; specific requirement for merosin in myotube stability and survival. *The Journal of cell biology*, 134(6), 1483 0021-9525.

Velleman, S. G. (2002). Role of the extracellular matrix in muscle growth and development. *American Society of Animal Science*(80), E8-E13.

Von Degenfeld, G., Banfi, A., Springer, M. L., & Blau, H. M. (2003). Myoblast mediated gene transfer for therapeutic angiogenesis and arteriogenesis. *British journal of pharmacology*, 140(4), 620-626 1476-5381.

Von der Mark, H., & Ocalon, M. (1989). The differentiation and redifferentiation of myoblasts is triggered by fibronectin and laminin. *Differentiation*, 40, 150-157.

Zisch, A. H., Lutolf, M. P., & Hubbell, J. A. (2003). Biopolymeric delivery matrices for angiogenic growth factors. *Cardiovascular Pathology*, 12(6), 295-310 1054-8807.